Climate Change and Integrating Hydrological-Crop Production Models driven by Remotely Sensed Data in the Guadalquivir Basin, Spain

June 2009

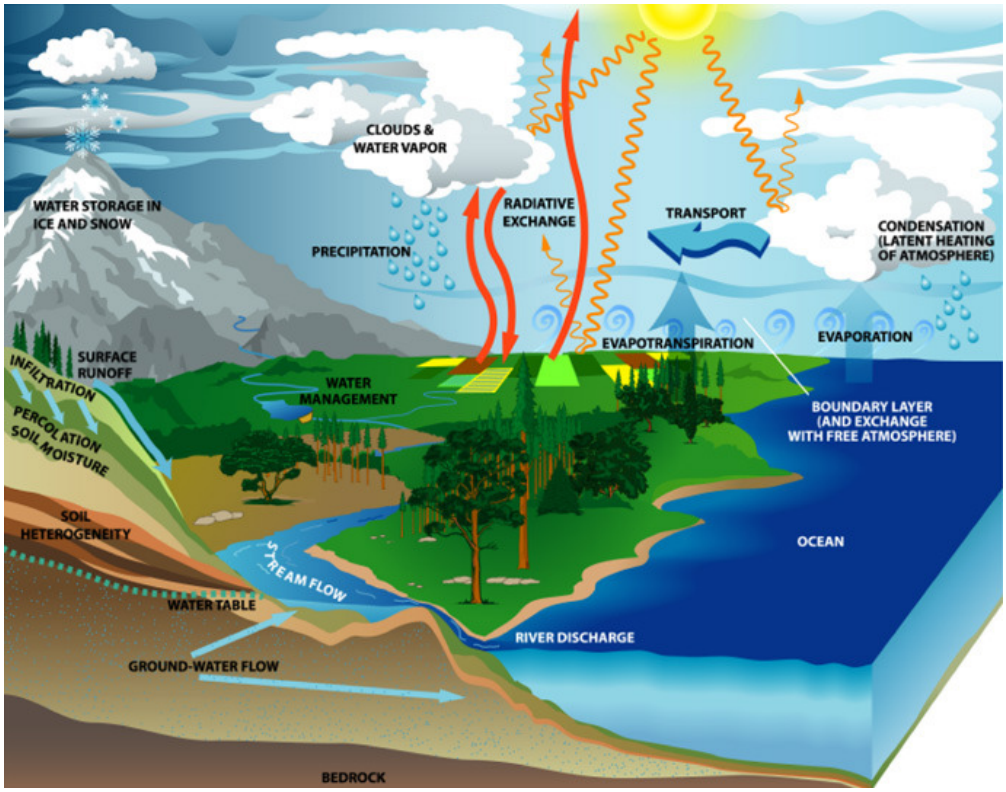

Author

Sameer Safaya

Supervised by

Dr. Walter Immerzeel

Dr. Marc Bierkens

FutureWater

Costerweg 1G

6702 AA Wageningen

The Netherlands

+31 (0)317 460050

info@futurewater.nl

www.futurewater.nl

Acknowledgements

This thesis project is the capstone of my 2-year Master of Science Degree in Hydrology as prescribed by the Geoscience College at Utrecht University. I would like to acknowledge Dr. Steven de Jong, as the professor of the remote sensing class I took at the UU, who introduced me to Dr. Walter Immerzeel, as he and I shared similar research interests. Dr. Immerzeel holds a position at the University and works for FutureWater, the company with whom I ultimately collaborated for this research project.

I'd like to acknowledge my faculty advisor Dr. Marc Bierkens for his guidance during this stage of my Msc career. Working with FutureWater was indeed a unique experience for me, and while it felt like an internship at times it was ultimately a research project in line with my interests, meeting the requirements of the Hydrology program and being of benefit to FutureWater themselves. I'm very glad to have had the opportunity of working at the office in Wageningen, and wish to thank Dr. Peter Droogers and all the other staff for making it a pleasant learning experience for me.

My biggest thanks are attributed of course to my direct thesis advisor, Dr. Walter Immerzeel, who was always supportive and patient. His uncanny ability to have an answer ready at all times, spoke volumes of his dedication and support towards my academic goals.

Finally I would like to thank those whose support and dedication has been unwaivering my entire life and that is my friends and loving family. My greatest gratitude goes to them for keeping me nourished mentally, physically and emotionally.

Table of contents

Summary

The objective of this investigation is to integrate remotely sensed precipitation and evapotranspiration data into a hydrological-crop production model and to compare the effects of model parameterization on the water balance at the catchment scale. The same region is then modelled with the effects of climate change and the resulting water balance evaluated for the end of the 21st Century. The study region is based in southern Spain, in the Guadalquivir basin and the specific data refers to the Genil-Cabra Irrigation Scheme (GCIS). Data from regional weather stations was used to feed the initial SWAT model, while remotely-sensed data was then used as a calibration tool to fine-tune the initial model via SEBAL (Surface Energy Balance Algorithm) until the modelled ET matched SEBAL ET. Water is fed from natural precipitation directly onto the land, irrigation systems and from further upstream. Reservoirs in the catchment act as an artificial delay of natural runoff. All natural streams and reservoirs were incorporated into delineating the extent of the sub-basins and the whole GCIS.

A sensitivity analysis revealed that the model was most sensitive to groundwater revaporation (a coefficient that determines how much water will be evaporated from the capillary fringe) and heat units (a summation of effective heat required by a plant to reach maturity). Thus these two parameters were varied and their respective annual outputs analysed per hydrological response unit (HRU). 127 HRU's were defined in the GCIS – plots of land each with their own unique combination of soil and crop types and other energetic and hydrological parameters. The results from the calibration were then compared to the original SEBAL data, which provided an estimate for regional annual evapotranspiration (ET).

For the calibration process a step-wise, forced iteration formula in MS Excel was used to manually calibrate the above parameters. The newly optimized parameters were then fed into the model again and an analysis was carried out on the basin which included all the water inputs and outputs to produce a final water balance for each HRU from January 2002 to August 2008. To create average reports only the complete years from 2002 to 2007 were ultimately used resulting in 464 mm of precipitation and 405 mm of ET on an annual average basis during this period. Some years receive significantly less rainfall such as 2007 which saw 364mm whereas others (2002) are wetter than usual receiving 551mm. Therefore the need for irrigation systems is justified to regulate the available water especially since ETp (potential evapotranspiration) is greater than precipitation. In 2004 the ETact (actual evapotranspiration) even exceeded the year's rainfall by 19mm. However one must not confuse the result of irrigation systems as increased water supply, since such systems merely tap into the same naturally available water but only distribute it more readily from upstream including the reservoirs to the agricultural areas where they are needed most. This may not be sustainable for the GCIS in the long-term as it quickens the delivery of already limited water supplies.

There are several ways to apply remote sensing to determine the water balance in a catchment. One can employ parameterization to significant detail and focus the subsequent model on specific parameters to achieve a best fit with satellite observations. Another option is forcing the model with rain radar information as in the tropical rainfall measuring mission (TRMM) or finally to use calibration and validation as is done here. In this study the efficacy of using remote sensing in previously ungauged basins was tested. The r^2 value of the calibrated model between SEBAL (satellite) based results and the SWAT (land) based results was 0.67.

Finally a climate change scenario is presented for the same region using IPCC reports for southern Spain using the forecasts for the end of the twenty-first century. With this data included in the model, one can then estimate the expected evapotranspiration under such conditions and the resulting water balance for the whole basin. Note that the use of discharges and reservoir systems leads to no real natural flow, but provides a good estimation of the overall water balance in the catchment.

Southern Spain in general experiences a typically hot and dry climate. With the additional forcing of climate change through global warming, evapotranspiration will be higher, and in other regions this may lead to more rain in fact. However in this region water is already limited and projected to be even dryer, with less rain and thus an increase of the need for systems much like the Genil-Cabra Irrigation Scheme. The climate of the late 21st Century will have an adverse effect on the water balance, groundwater processes and ultimately on crop yields and the GCIS may no longer be sustainable for the 22nd Century and beyond. The 100 year projections yielded an increase in temperature and a decrease in rainfall resulting in a water balance with 406 mm of precipitation and 353 mm of ETact as the annual average. A future with 12.5% less rainfall has significant impacts on local crop production and planting schedules as well as an overall decrease in aquifer recharge by a further 47%.

Using previously mentioned techniques should ultimately help in estimating the level of the groundwater table without any intrusive methods such as the drilling of boreholes. It takes much time, energy and resources to drill boreholes for monitoring the water table across a landscape. Therefore, to be able to have a good idea of the groundwater levels in a basin without ever traveling to such locations is a great advantage for planners and resource managers alike. Calibrating models using remote sensing is much more effective and economical than using expensive monitoring systems. Using geologic maps in conjunction with methods similar to those mentioned in this paper, one can have a good understanding of the sub-surface system which enables mankind to make better use of such a vital commodity.

In this study unfortunately, no groundwater data was available from the Spanish partners to confirm or reject the model's estimation of the height of the water table as it is produced as a residual from the overall water balance for each HRU. However, with initial levels assumed and the various water fluxes considered, the patterns of seasonal variability are indeed noticeable and their respective levels within the realm of reasonable estimation.

1 Introduction

1.1 Problem statement

Climate in the Mediterranean experiences dry summers and wetter winter and spring seasons, thus growing crops in this region is heavily dependant on irrigation systems, where water availability is highly variable between years. With increasing food demand and scarce water supplies, the need for optimal water use is critical for maintaining the health of the crop and a timely harvest. The effects of climate change are felt here with an increasing frequency of drought, and hotter summers, thus sustainable water use is increasingly necessary. According to the IPCC's fourth assessment the southern Mediterranean will experience up to 24% less rainfall and 4.1°C increase in temperatures when comparing the end of the 20th century with the end of this century and looking at median quantiles for the projections. (See Table 1 below).

Table 1. Regional averages of temperature and precipitation projections from a set of 21 global models for the A1B scenario adapted from the IPCC 4th Assessment. (IPCC, 2007).

		Temperature Response (°C)						Precipitation Response (%)						Extreme Seasons (%)		
Region[a]	Season	Min	25	50	75	Max	T yrs	Min	25	50	75	Max	T yrs	Warm	Wet	Dry
SEM	DJF	1.7	2.5	2.6	3.3	4.6	25	-16	-10	-6	-1	6	>100	93	3	12
	MAM	2.0	3.0	3.2	3.5	4.5	20	-24	-17	-16	-8	-2	60	98	1	31
30N,10W	JJA	2.7	3.7	4.1	5.0	6.5	15	-53	-35	-24	-14	-3	55	100	1	42
to	SON	2.3	2.8	3.3	4.0	5.2	15	-29	-15	-12	-9	-2	90	100	1	21
48N,40E	Annual	2.2	3.0	3.5	4.0	5.1	15	-27	-16	-12	-9	-4	45	100	0	46

According to Working Group 2 of the 4th Assessment (IPCC, 2007) there are several vulnerabilities and impacts to consider for the Mediterranean region in the years to come. It is said with high confidence that warmer, drier periods will lead to more droughts and a longer fire season with increased fire risk. Crop productivity is likely to decrease in the Mediterranean and in south-east Europe – this includes the retreat of forests and an acceleration of tree mortality. Projected water stress will increase in the region seeing a rise from 19% today to 35% by 2070 where summer flows may drop by 80% affecting millions of people. This will also result in the decline of hydropower production by 20-50%. Ecosystems are also threatened as the species within them may not able to adapt as quickly to the changing environment. Many ephemeral aquatic ecosystems are projected to disappear whilst more permanent ones are expected to shrink. There is also said to be a decrease in annual runoff - up to 20% in southern Europe. In coastal regions there is always the risk of sea-level rise and by 2080 according to the A1F1 climate scenario the Mediterranean population is also at risk by flooding (IPCC, 2007). Hence the need to model water systems with a changing climate and test their sustainability.

The Genil-Cabra Irrigation Scheme in southern Spain was selected for this study as FutureWater has partners in the region who have been collecting data for years. This level of history and detail from a hydro-meteorological perspective was well suited for this undertaking as the models are data intensive as well as spatially and temporally sensitive.

1.2 Literature Review

A paper titled the “Calibration of a distributed hydrological model based on satellite evapotranspiration” by Immerzeel and Droogers (2007) describes an innovative process using remotely sensed-derived evapotranspiration in the calibration of SWAT for a catchment in the Krishna basin in southern India. An application of the Gauss-Marquardt-Levenberg algorithm was detailed for the optimisation of various combinations of soil, landuse, meteorological and groundwater parameters. These led to an increase in the r^2 relation between monthly sub-basin simulations and ETact from 0.40 to 0.81. From this study it appears that ETact was more sensitive to the groundwater and meteorological parameters than those of soil or landuse. It surmised that further study would be required at a spatial resolution below the sub-basin level to fine tune the calibration procedure. Direct measurement of evapotranspiration is possible via lysimetry and while this may be most accurate, it is quite difficult to cover an entire catchment in such a way. One would suspect ground measurements to be more reliable and direct than satellite-derived readings, however it appears in general SEBAL has been rigorously examined; thus SWAT is being calibrated by SEBAL rather than the other way around and it is much better suited to use satellite readings at the catchment scale. However it should be noted that SEBAL assumes the evaporative fraction to be constant all day and this of course is only suitable in regions where this is indeed true (such as subtropical-equatorial climates). Also no direct precipitation data was incorporated into their study. Rainfall measurements in their case were derived using the TRMM satellite at a coarse resolution of 25km and scaled accordingly to fit the grid and even then a weather generator was employed since no long-term statistics on daily rainfall distributions were available.

Furthermore the landuse input of the SWAT model is also in question in the above paper. It was based on 15 unsupervised classes based on a time series of 16 MODIS images using NDVI filters at a resolution of 250m. These were then confined to 6 classes based on existing maps, field surveys and high resolution satellite imagery for verification. However the final landuse map produced does not provide enough detail in the type of agricultural crop grown. The final classes were low/high density forest, irrigated/supplemental/rainfed agriculture, rangelands and water. The forest and rangeland classes are reasonable, however the rest is not, especially when considering the large size of the catchment (of which roughly 70% is agriculture) and the influence particular crops would have on the overall water balance.

Immerzeel and Droogers (2007) make use of PEST and go into much detail assessing AWC, BLAI, RFINC and GWREVAP parameters. (See appendix for graphs of parameter sensitivity analyses). The goal of PEST is to minimise the objective function which is defined as the sum of squared deviations between model outcomes and experimental observations. The objective function is closely related to the commonly used root mean square error.

In another paper entitled “Integrating remote sensing and a process-based hydrological model to evaluate water use and productivity in a south Indian catchment,” Immerzeel et al.

(2007) combine the use of remote sensing and a distributed hydrological model to improve the understanding of water balances in data scarce areas. Likened in many spatial and temporal aspects to the former paper under review, such as FAO soil maps and similar land-use classes, its main difference includes the use of actual meteorological data from weather stations as opposed to TRMM derived precipitation. It also goes into the HRU level to calculate the water balance, considers streamflow data in the routing network and biomass production.

The paper outlines three types of crop-water productivity: technical, economic and socio-economic water productivity. That is the mass of product, net private benefits and net social benefits per unit of water consumed respectively. The focus was mostly on the first technical point and based productivity on the ratio of yield and ETact. SWAT was intermittently validated with SEBAL during the year long study; however this was not possible for over half the year due to monsoonal cloud cover so the calibration may be skewed for this period. The paper does admit to a significant decrease in storage over the period of the study and attributes this to a number of factors which center on data limitations and thus warrant further research.

In my investigation a similar approach is being undertaken for a different catchment except the SWAT model is running below the sub-basin level down to the HRU level and is therefore more refined but also applied to a different catchment (southern Spain instead of India). Here, weather station data is provided so rainfall need not be estimated via satellite and the landuse classes are numerous and well defined. During parameterization only two parameters were being optimised in this study. It was thereby determined that a step-wise forecast function in excel was sufficient for the optimisation.

A paper titled “Integrating satellite-based evapotranspiration with simulation models for irrigation management at the scheme level,” by C. Santos, I. J. Lorite, M. Tasumi, R. G. Allen, E. Fereres (2007) offers good reference material since it is based in the same region as this investigation. It employed a good temporal and spatial concept using daily derived soil-water balance readings by instrumentation and high spatial resolution by satellite remote sensing to cover the whole catchment and formed the basis of the methodology used in this study. Remote sensing techniques have been recently developed for the estimation of ET using surface energy fluxes and have been well validated in other regions as well by lysimetry (Tasumi et al. 2005b), such as the use of METRIC (Mapping EvapoTranspiration with high Resolution and Internalized Calibration) in western USA, (Allen et al. 2005a, 2007b).

For these reasons the approach to estimate the water balance by residual energy calculations, deriving ET from satellite remote sensing in conjunction with instruments on the ground, (whose parameters are then calibrated by the satellite data) seemed ideal for this study. It provides a high spatial and temporal resolution which would not be possible by lysimetry or other methods alone to measure ET on the catchment scale.

1.3 Justification

In order to optimize existing practices of irrigation, crop growth potential and hydrological models are needed; however a lack of ground data translates to the use of evaporation as an alternative model input. Field techniques have been employed in the past to measure ET; however this is only appropriate at the local plot scale that is within the proximity of the individual instruments. Estimates of ET at regional scales are most commonly done now via remote sensing. These systems estimate ET based on energy balance algorithms such as SEBAL. The balance involves incoming solar radiation, which is measurable on the surface, the ground heat flux, sensible heat and latent heat (the energy required to evaporate water). Emissivity of the soil, which is in turn a function of surface temperature and moisture, can also be found via satellite RS and is important in the energy balance equation and ultimately in the water balance of the system.

1.4 Hypothesis and research questions

In this study a commonly used water management and crop production model will be tested and compared with parallel data produced by the MODIS satellite. By calibrating the model with remotely sensed evaporation fields, the land-water balance can be estimated and irrigation schedules optimised. The model to be set up is the Soil and Water Assessment Tool (SWAT) and it is a (semi-) distributed model. The objective of this research is to set up a SWAT (in 2-D mode) and for specific hydrological response units (HRU) in the Genil–Cabra Irrigation Scheme and compare the effects of parameterization in the model on the water balance and crop production. For this purpose a representative agricultural plot will be selected and the models will be driven by remotely sensed data and then compared with SEBAL (Surface Energy Balance Algorithm).

Upon setting up the SWAT model, the water balance can be estimated at various scales from individual HRUs to the whole basin. The aim is to recreate a similar outcome with the data driven by SEBAL. Although there is a shift in resolution when using SEBAL data, one can still select appropriately sized HRU's to match this new resolution and thus make for a fair comparison regarding the model outputs. Having done a preliminary climate variation analysis across the basin and within the GCIS one can see this correlation being fairly reasonable. Climate data from within the GCIS (Santaella) does indeed agree with that recorded by meteorological stations from surrounding cities as well except perhaps during summer months. (See figure 4).

The main research questions are: whether a SWAT model can be calibrated on ET - ie. the efficacy of using remote sensing in previously ungauged basins (PUBs); what is the water balance of the GCIS and the subsequent crop production; what are the effects of climate change on the local water balance and its implications for the future.

1.5 Report outline

Chapter 2 describes the study area in detail with references to both the Spanish classification systems and general observations. Chapter 3 describes the general setup of the investigation: A discussion of SWAT and the model parameters themselves will follow and the subsequent methodology will be detailed as well. The SWAT model is built on the inputs from the various weather stations situated across southern Spain in the Guadalquivir basin. Daily readings from 2002-2008 which measure insolation, precipitation, temperature, relative humidity and wind were used. IFAPA provided the detailed soil and landuse maps for the GCIS as well as the 250m DEM. SEBAL data was also made available for the same region and one specific year (2004-2005) was investigated more closely since it was one of the driest since 2002.

Chapter 3 continues to describe SWAT and how it models the GCIS to produce the water balance and resulting crop growth at the HRU level within the catchment. The resulting ETact is then calibrated against SEBAL derived ETact. Before calibration, a sensitivity analysis revealed that groundwater revaporation and heat units were the most appropriate parameters to improve on. This was carried out through MS Excel's forecast function within an acceptable range of values. The experiment was then repeated, however this time using the calibrated model with a projected climate input for the region provided by the IPCC for the end of the 21st century, thus a climate change scenario is simulated and a comparison is made. This has impacts on both the region's water balance and of course its crop production and will be analysed in the results and discussion section of the paper which can be found in Chapter 4.

The results and discussion section presents ET by SWAT and SEBAL, both spatially and temporally and is compared for discussion purposes. Whilst SEBAL has been clearly validated from previous literature (Bastiaannsen, et. al 1998) it does pose the question, which one is correct? Since SEBAL does not include a crop growth model it can only be used for water balance comparisons which will ultimately only be validated by ground-truthing.

From the investigation a variety of conclusions can be drawn and these are featured in Chapter 5. This is followed by an evaluation that will reflect on the work thus far, including comments on future improvements and recommendations and this is found in Chapter 6.

The full reference list follows in Chapter 7 ending with an appendix as Chapter 8 which shows selected calibration results with the best fit between SEBAL measured and SWAT estimated ETact.

2 Study area

2.1 Guadalquivir

The Guadalquivir is the fourth longest river in Spain (after the Tagus, Ebro and Douro), and the longest in Andalusia (*Figure 1*). The name comes from the Arabic al-wādi al-kabīr, 'The Great River'. The Guadalquivir is 657 kilometers long and drains an area of about 58,000 square kilometers. It begins at Cañada de las Fuentes in the Cazorla mountain range (Jaén), passes through Córdoba and Seville and ends at the fishing village of Bonanza, in Sanlúcar de Barrameda, flowing into the Gulf of Cádiz, in the Atlantic Ocean. The marshy lowlands at the river's end are known as "Las Marismas". The Guadalquivir River is the only great navigable river in Spain. Currently it is navigable up as far as Seville, but in Roman times it was navigable to Córdoba.

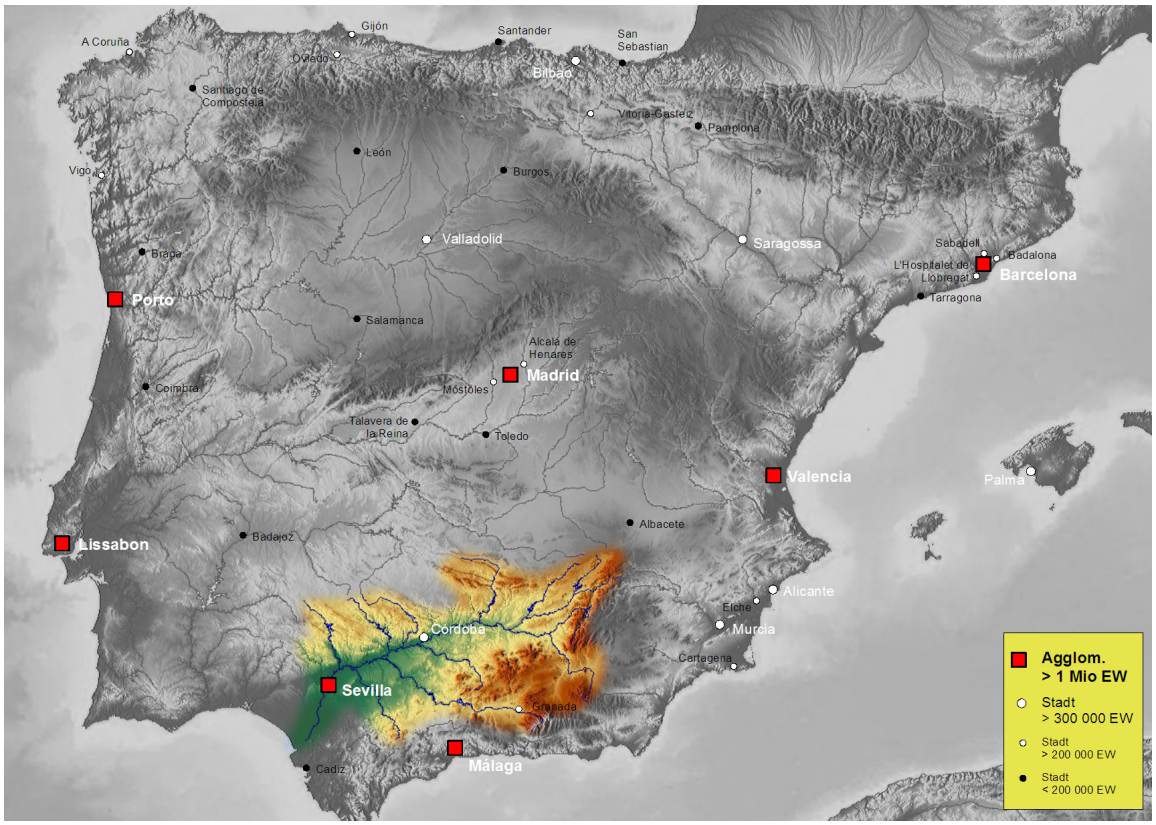

Figure 1. Location of Guadalquivir (source Wikipedia and http://www.maps-for-free.com/)

Most important tributaries of the Guadalquivir river are (see Figure 1 above):
- left; Guadiana Menor, Guadalbullón, Guadajoz, Genil, Corbones, Guadaira
- right; Guadalimar, Jándula, Yeguas, Guadalmellato, Guadiato, Bembézar, Viar, Rivera de Huelva, Guadiamar.

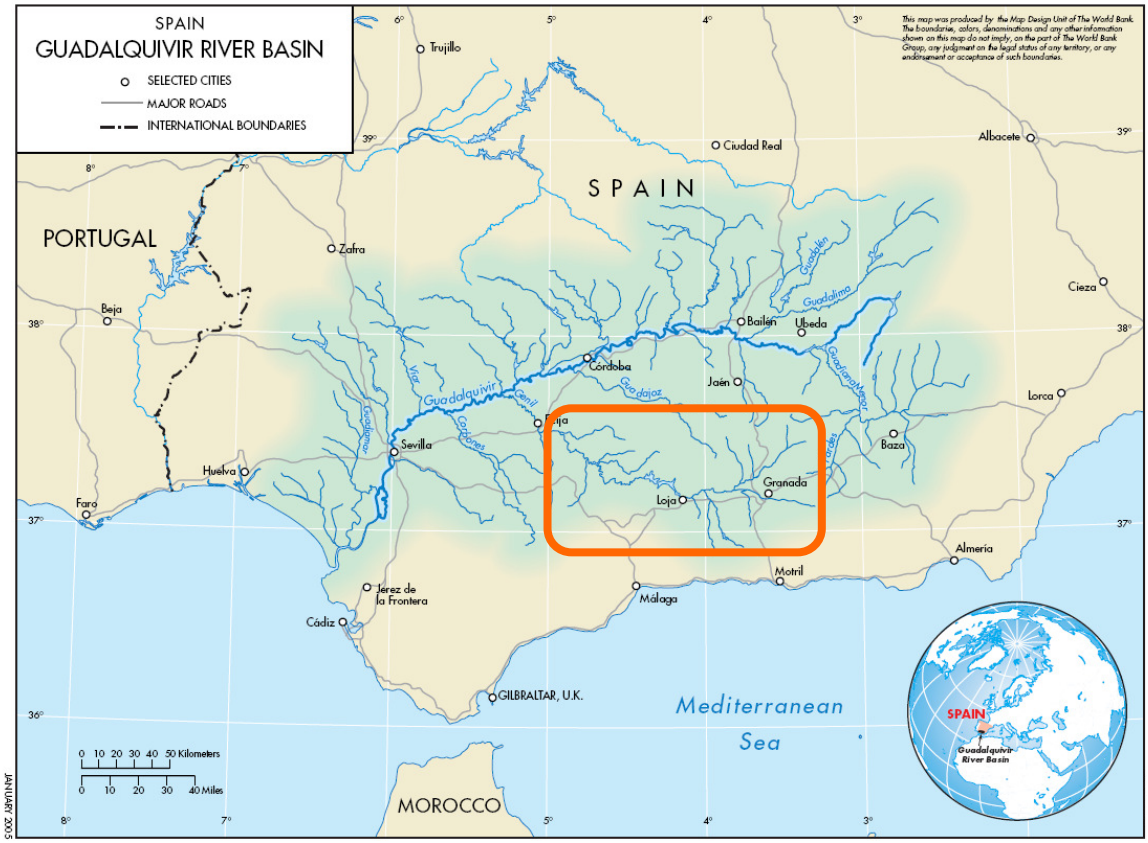

Figure 2. Guadalquivir river and its tributaries and the study catchment of the Genil and Cabra Rivers, (Blomquist et al., 2005).

Based on altitudes, soils, runoff coefficients and groundwater existence, the basin is commonly subdivided into three main geomorphologic units:

- The Sierra Morena (maximum altitudes of 1000 m) in the northern part of the basin. It is generally composed of impermeable primary rock.
- The Sistema Betico, on the left bank of the Guadalquivir, with the highest altitudes of the Iberian peninsula (>3,000 m), where the main left bank tributary of the Guadalquivir River flows, i.e. the Genil river.
- The Guadalquivir River depression, which has altitudes lower than 100-200 m. The plain around Seville has an altitude between 0-6 m, at a distance of 80 km from the mouth of the river: this confers to this last stretch of the river its characteristic meandering nature.

The Confederación Hidrográfica del Guadalquivir uses a somewhat more refined division in five zones (*Figure 3* and Table 2).

Table 2. Geophysical zones.

Name	Population	Area (km^2)
Sierra Morena	328,979	18,409
Campiñas y Vegas	2,495,910	17,99
Sierras Béticas	386,896	12,24
Depresiones Intrabéticas	589,77	6,289
Litoral	15,784	1,179
TOTAL	**3,817,319**	**56,107**

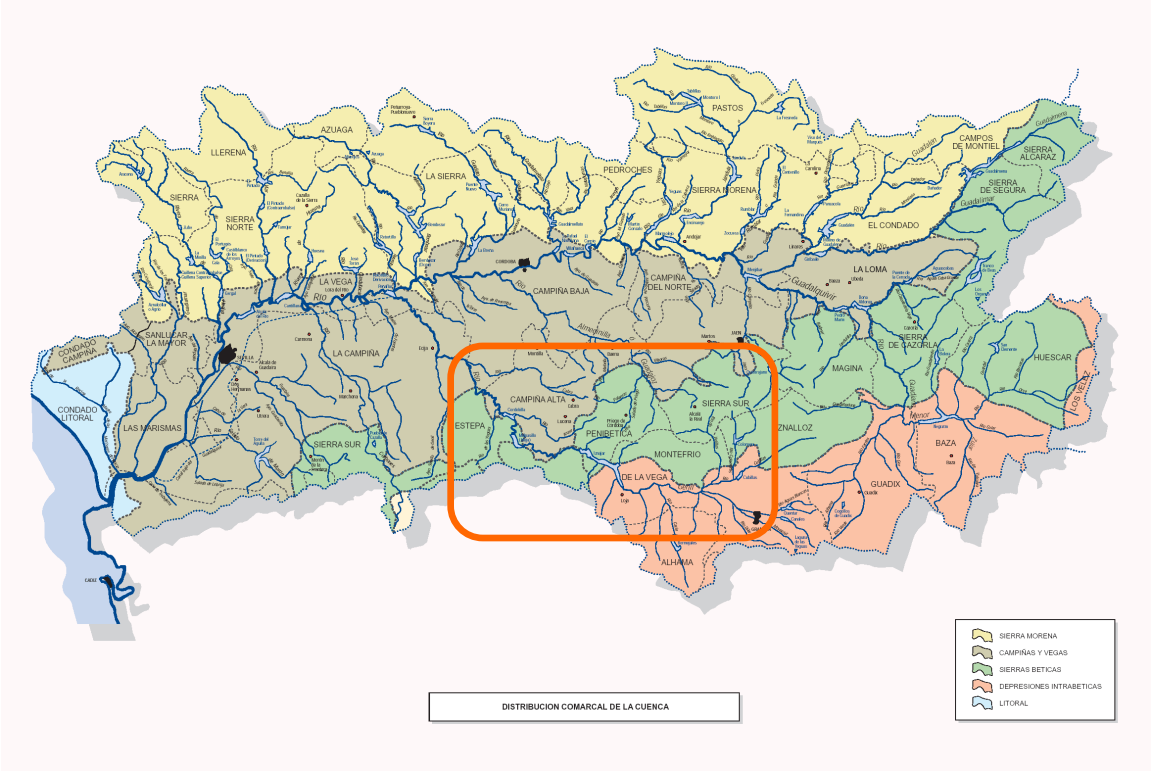

Figure 3. Main morphological zones within the Guadalquivir basin, the Genil-Cabra basin which is the study catchment is in the orange box.

An even more detailed zonal system has been defined as well by the Confederación Hidrográfica del Guadalquivir and is used for their water resources planning. The system consists of the following divisions:

- Zones (5)
- Subzones (20)
- Areas (48)
- Hydrological Units (300)

The study region investigated here occurs in the grey and green zones shown above, that is the “Campinas Y Vegas” and the “Sierras Beticas” zones respectively.

2.2 Study Catchment and the GCIS

This project is based on data derived from the Guadalquivir Basin in southern Spain, and is specifically centered on an area known as the Genil-Cabra Irrigation Scheme. The GCIS is fed by several smaller rivers and reservoirs within a catchment area of 7215 km². The climate is typically Mediterranean, that is very hot and dry summers and mild, wetter winter and spring seasons, experiencing an average annual rainfall of 491mm between the years 2002-2008 with temperatures ranging from 8-28 degrees C (avg. of 17.6 degrees C).

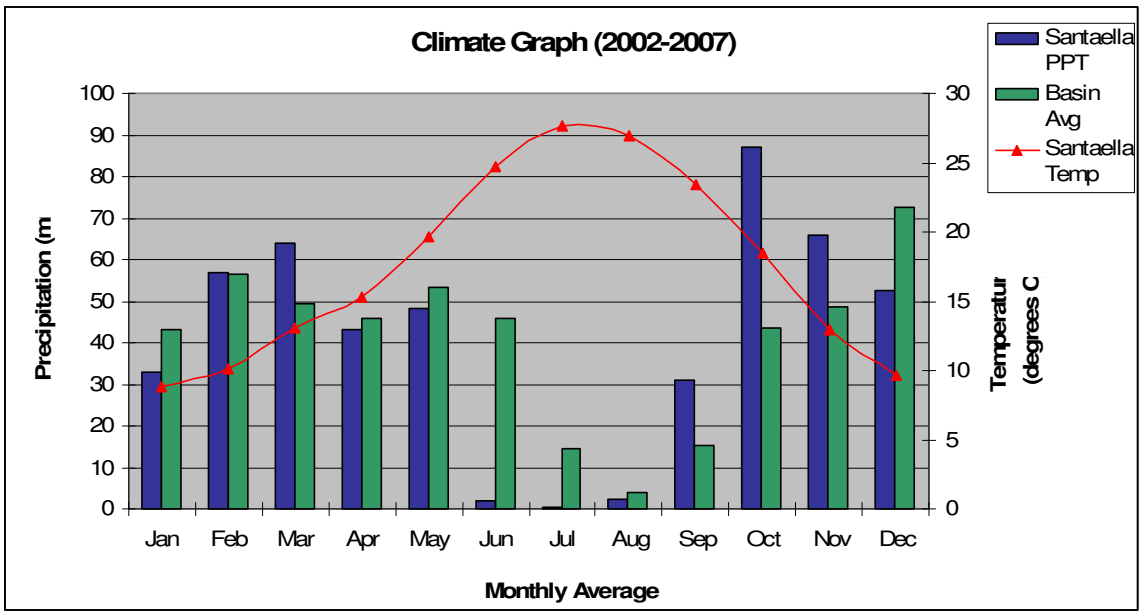

Figure 4 – Basin Average Climate Graph

The above graph shows the climate data of all the stations used in this study and for quick comparison purposes, the average basin precipitation is compared with the GCIS (Santaella) precipitation data. The precipitation values are fairly similar except for June and October. The temperature data is fairly comparable for the whole region so only one line (in red) is given to represent the regional temperature conditions.

Within the catchment area the local landuse is focused primarily on agriculture with some forested areas prevalent as well. The most popular crops include olives, winter wheat and other irrigated agricultural products. The topography is undulating with higher lands up to 3420m to the east, which gradually flatten out to 101m in elevation towards the west, and thus the resulting streams flow similarly in orientation. Within the GCIS itself however the altitude varies only slightly from 120-230m above sea-level, producing limited slope. Six types of predominant soils have been identified in the watershed, varying from clay types to more sandy compositions (see Table 3 below). The various soils change the nature in which water flows depending on their inherent properties like structure, conductivity, porosity, moisture, grain size etc.

Table 3. – Soil Types in the Genil-Cabra Basin (FAO, 1995)

Soil ID	Code	Type	Ksat (m/yr)	Depth (cm)	Area (Ha)	%Basin
7	Bk47-2/3b	silty clay loam	49.8	115	554187.50	76.81
14	Be120-2bc	silty clay loam	55.0	75.5	6537.50	0.91
26	Wd5-1a	sandy clay loam	175.4	125	23856.25	3.31
30	Lc106-2b	clay loam	92.6	72.5	101006.25	14.00
33	Vc14-3a	silty clay	17.9	125	21318.75	2.95
35	Vp68-3a	clay loam	83.7	125	14575.00	2.02

Land-use or cover type plays an extremely important role in developing a hydrological model since it has a direct impact on the physical processes that drive the water cycle. Each crop type has a different transpiration rate, leaf area index, life cycle, root depth, etc. and each of those properties has impacts on the water balance, thus the more information available, the more accurate the model will be. Listed below are the 14 cover types in the Genil-Cabra basin including the GCIS and their respective areas.

Table 4. – Land-use Types and Area

Land-Use	Abr.	Area (Ha)	% Basin
Winter Wheat	WWHT	3518.75	0.49
Corn	CORN	550.00	0.08
Sugarbeet	SGBT	506.25	0.07
Green Beans	GRBN	237.50	0.03
Irrigated Agriculture	AGRI	5412.50	0.75
Bare Lands	BARE	25.00	0.00
Olives	OLIV	311437.50	43.17
Onion	ONIO	500.00	0.07
Eggplant	EGGP	25.00	0.00
Sunflower	SUNF	137.50	0.02
Alfalfa	ALFA	31.25	0.00
Agricultural Land-Generic	AGRL	232887.50	32.28
Range-Brush	RNGB	134143.75	18.59
Forest-Deciduous	FRSD	32068.75	4.44

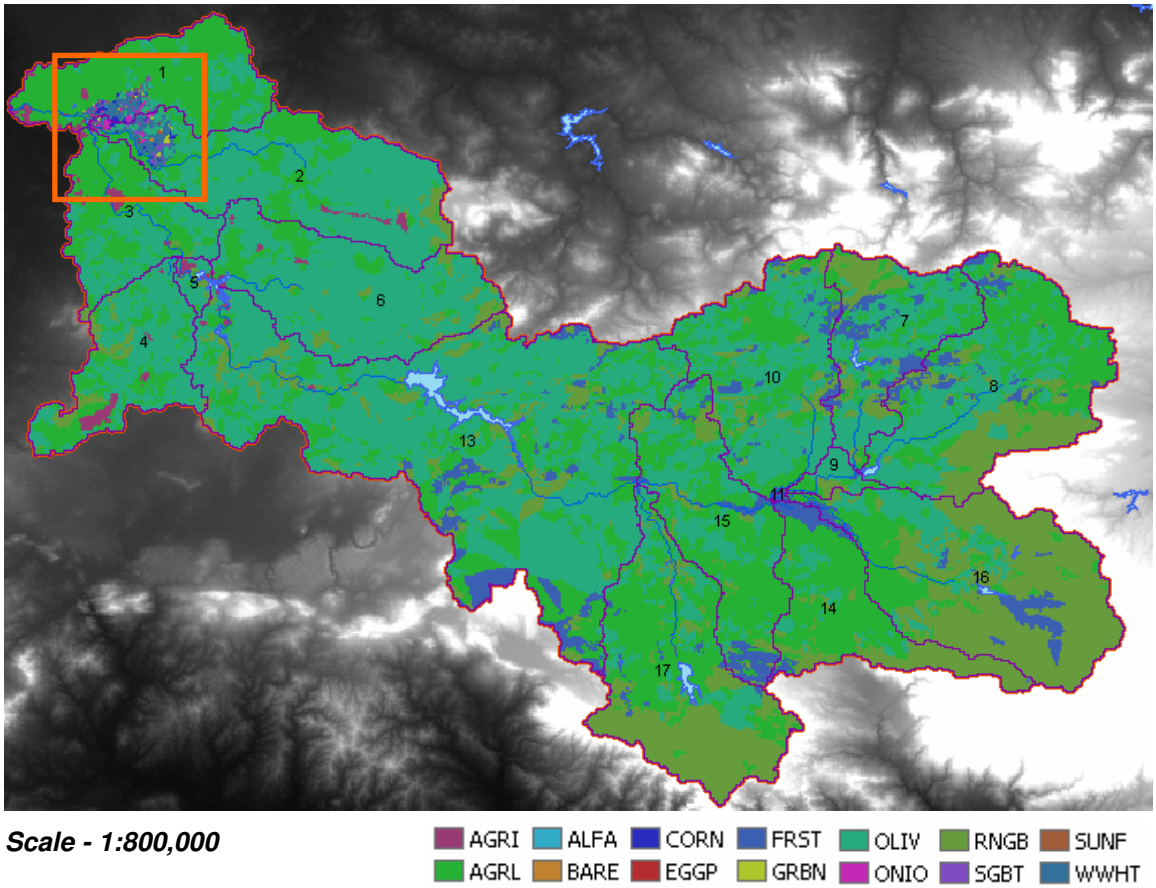

Scale - 1:800,000

Fig. 5 – Genil-Cabra Catchment (DEM 250m) divided into its 17 sub-basins with an orange square marking the GCIS itself. Reservoirs and streams are also visible in light blue.

NB: Of the five meteorological stations, only Santaella's is found within the GCIS, but the others are situated proximally to the catchment so are indeed appropriate for use in this investigation.

Fig. 6 – FAO Soil Map with GCIS outlined in black in the NW corner.

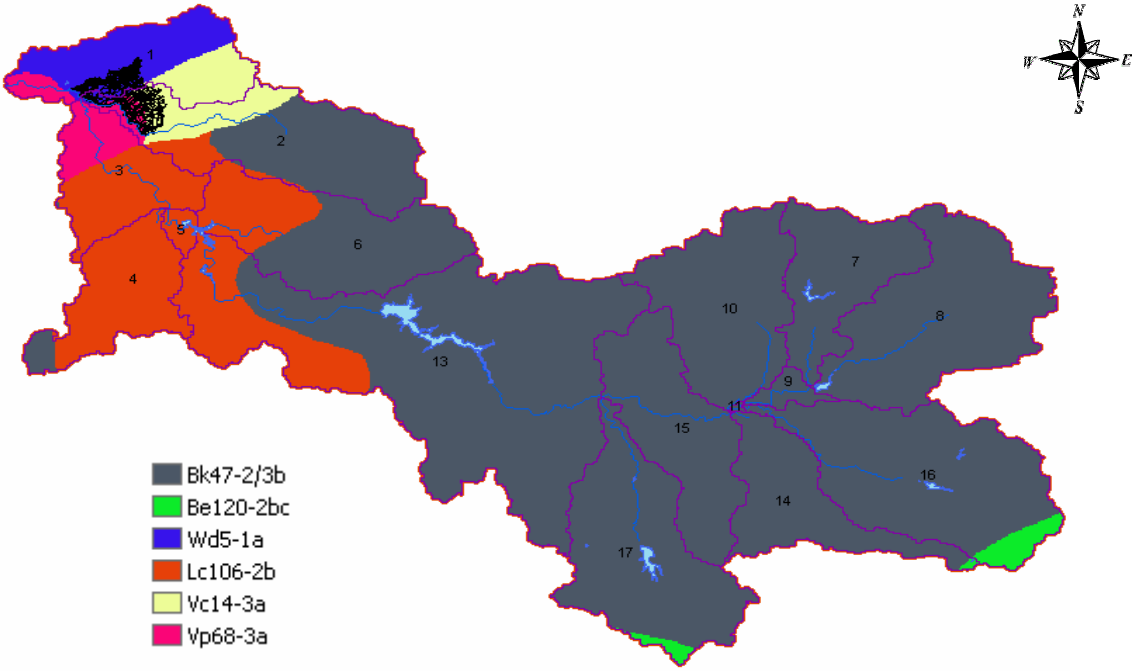

3 Methodology

3.1 General

Process Flow

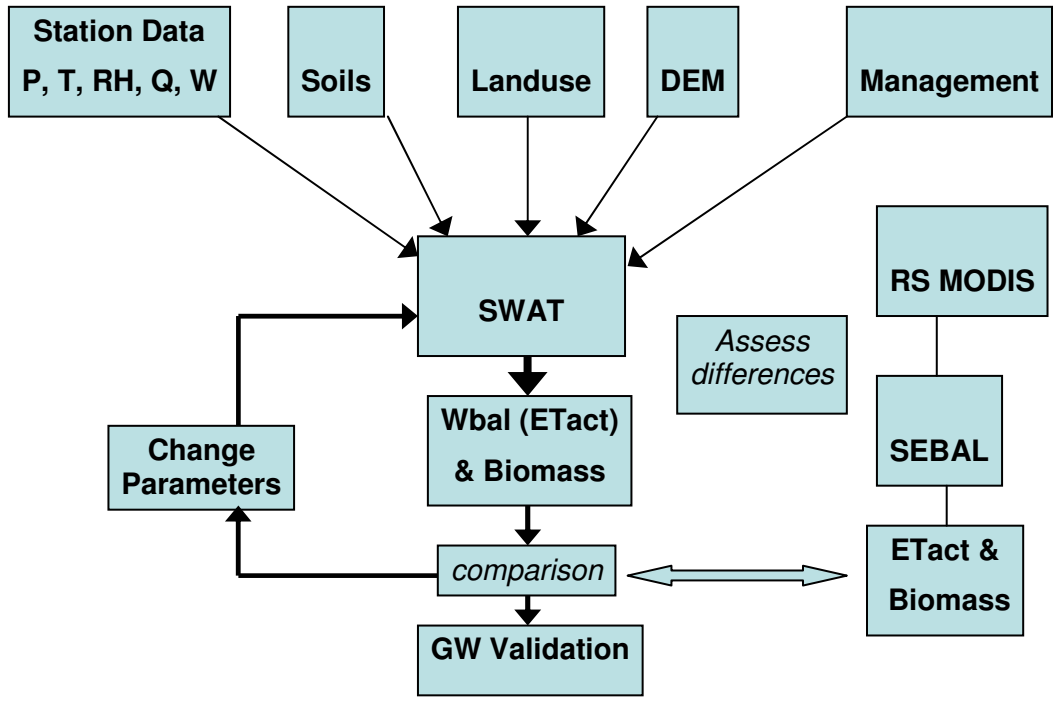

Fig. 7 - Methodology Flow chart

The chart above shows the process flow of the entire study from inputs into models to result comparisons and calibration and serves as a summary to the methodology which is described in detail shortly. The data garnering process began with weather stations across 5 cities that encompassed the region of study; each provided precipitation, temperature, relative humidity, insolation and wind information from 2002-2008. Then soil data of the GCIS was provided by the Spanish partners together with the plots' respective land uses - management practices are also setup accordingly, such as irrigation schedules. A 250m digital elevation model of the entire catchment is also fed into the SWAT model thus providing the final critical input to generate a drainage basin with defined catchment boundaries. RS data was provided by FutureWater.

3.2 SEBAL

3.2.1 Theory

SEBAL or the Surface Energy Balance Algorithm for Land (Bastiaanssen, 1998), uses spectral radiances recorded by satellite-based sensors, as well as basic meteorological data, to

solve the energy balance at the earth's surface. Its primary outputs are water consumption, or actual (not reference or potential) evapotranspiration (ET_{act}), and biomass production of agricultural crops and native vegetation, pixel by pixel. For some crops, yield can be reliably inferred from biomass production.

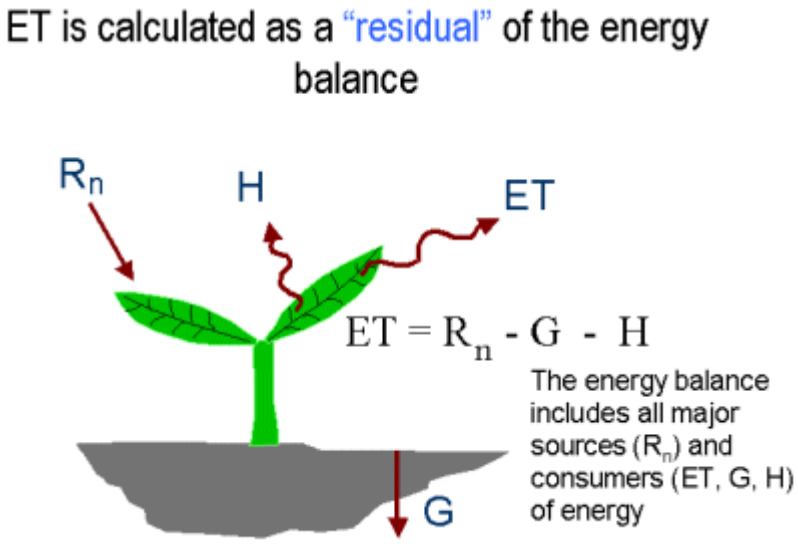

Fig. 8 – Energy Balance equation – Source (www.sebal.us)

SEBAL was refined into METRIC (Allen, 2007) for applications in mountainous terrain and to incorporate internal calibration to land-based reference evapotranspiration. SEBAL applies radiative, aerodynamic, and energy balance physics in a series of 25 computational steps whereby evapotranspiration is computed as a residual of the surface energy balance. Knowledge of land use and crop types is not needed, since all information, with exception of ground-based weather data, is obtained from the satellite image. In a sense it incorporates all the coverage data from radiance. The calculation of ET_{act} is for a large part driven primarily by the thermal channels of the satellite sensor. By solving the energy balance for a "dry" and "wet" pixel, SEBAL bypasses the absolute calibration of the thermal channels.

Instantaneous and daily ET_{act} and biomass production outputs are computed directly by SEBAL. These results can be extrapolated to longer time periods of weeks or months using ratios of ET_{act} from SEBAL to reference ET computed from ground-based weather stations. Integration over time provides accurate seasonal and annual estimates of ET_{act} and biomass production with the same spatial resolution of the source image.

3.2.2 SEBAL application in the GCIS

The SEBAL model was applied for the Guadalquivir basin to quantify weekly actual and potential evapotranspiration and biomass production. The hydrological year running from October 2005 to September 2005 was selected as this year was extremely dry and experienced serious water shortages. The SEBAL model was applied on MODIS images with a resolution of 1 kilometer. These images are used to derive the surface albedo, surface temperature and the

Normalised Difference Vegetation Index. Besides these satellite products, the SEBAL model requires spatial inputs of four standard meteorological parameters: air temperature, relative humidity, wind speed and solar radiation. These measurements were obtained from meteorological stations in the study area. The spatial interpolation of the point measurements was conducted with the MeteoLook tool that includes surface characteristics, such as surface roughness, vegetation cover and elevation, in the interpolation. Other inputs required here are a digital elevation model (DEM) and a land use map to derive surface roughness.

3.3 SWAT

3.3.1 Theory

The water balance results from all the hydrological processes that occur in the watershed. The simulated hydrology of a watershed can be separated into two major components. The first division is the land phase of the cycle depicted in figure 9. The land phase of the hydrologic cycle controls the amount of water, sediment, nutrient and pesticide loadings to the main channel in each sub-basin. The second division is the water or routing phase of the hydrologic cycle which can be defined as the movement of water, sediments, etc. through the channel network of the watershed to the outlet.

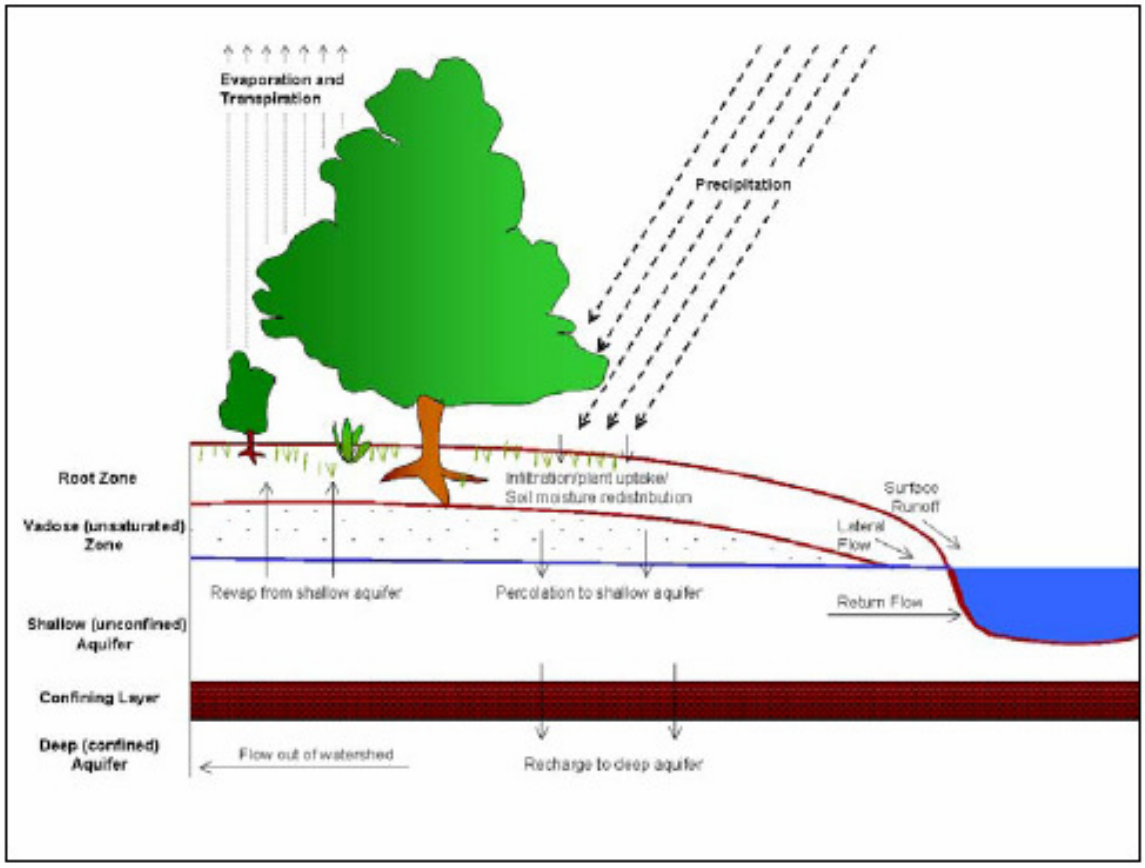

Figure 9 – Water Balance featuring inputs, outputs and changes in storage

The land phase of the hydrologic cycle is simulated by the SWAT model based on the following water balance equation:

$$SW_t = SW_o + \sum_{i=1}^{t} (R_{day} - Q_{surf} - E_a - W_{seep} - Q_{lat} - Q_{gw})$$

where SW_t is the final soil water content, SW_o is the initial soil water content, t is the time (days), R_{day} is the amount of precipitation, Q_{surf} is the amount of surface runoff, E_a is the amount of evapotranspiration, W_{seep} is the amount of water infiltrating the vadose zone, Q_{lat} is the water that flows laterally through the soil and Q_{gw} is the water that percolates down and finally contributes to the ground water flow. All amounts are given in mm H_2O and on day *i*.

Subdividing the watershed as above and into sub-basins allows the model to highlight differences in evapotranspiration for various crops and soils. The watershed is subdivided further into individual and unique HRU's, thus runoff is predicted separately for each HRU and routed to obtain the total runoff for the watershed. This will increase the accuracy and provide a significantly more astute description of the water balance.

To build a SWAT model, one would require temporal data such as daily precipitation, maximum/minimum air temperature, solar radiation, wind speed and relative humidity. The model allows for these values to be input from actual observed data records or from a weather generator during simulation. The latter produces weather data from average monthly values for each sub-basin and there is no spatial correlation of generated values from one sub-basin to the next. Snow is also considered differently since precipitation is governed by the average daily temperature. In addition, SWAT considers the DEM, land cover and shading to allow for non-uniform snow cover thus affecting the temporal and spatial aspect of snow melt.

SWAT Model Schematic:

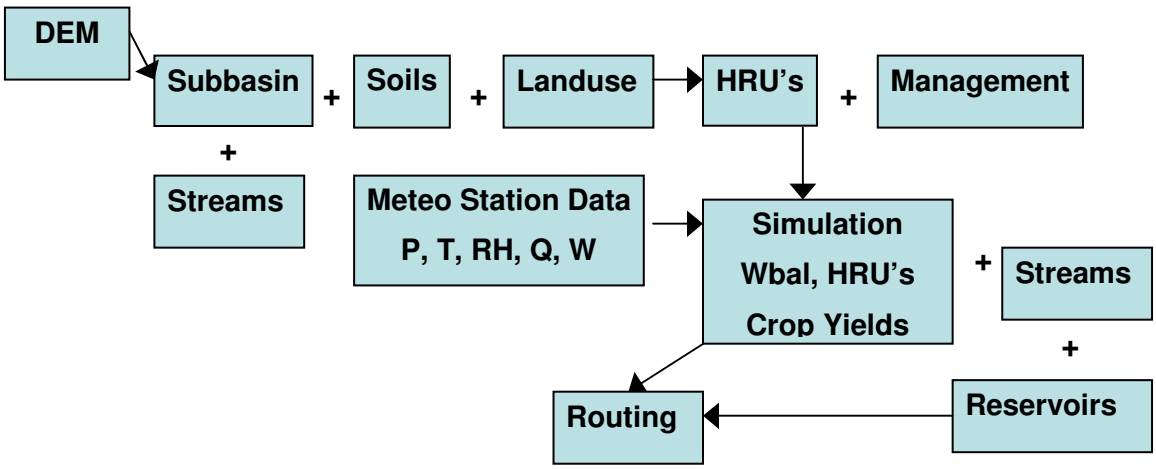

P – Precipitation, T – Temperature, RH – Relative Humidity, Q – Radiation, W - Wind

As precipitation falls or snow melts, it may be intercepted by the vegetated canopy or continue to the soil surface. Surface water will either infiltrate into the soil profile or continue to flow as runoff, the latter of which would contribute runoff more quickly towards the stream channel. Water in the shallow surface may be evapotranspired, held in the soil profile or may ultimately percolate down to the water table as depicted in figure 9.

One of the central points of discussion in this study is evapotranspiration, and potential ET was first introduced by Thornthwaite (1948) as part of a climate classification scheme. It was defined as the maximum amount of water that could evapotranspire from an area that shared uniform vegetative cover and unlimited water. Penman-Monteith (1956) developed an equation to account for the energy needed to sustain evaporation, wind strength and aerodynamic resistance terms and these are also incorporated into the SWAT model:

$$\lambda E = \frac{\Delta \cdot (H_{net} - G) + \rho_{air} \cdot c_p \cdot [e_z^o - e_z] / r_a}{\Delta + \gamma \cdot (1 + r_c / r_a)}$$

where λ is the latent heat of vaporization (MJ/m³/d), E is the depth rate evaporation (mm/d), Δ is the slope of the saturation vapour pressure-temperature curve (kPa/℃), H_{net} is the net radiation (MJ/m²/d), G is the heat flux density to the ground, ρ_{air} is the air density (kg/m³), c_p is the specific at constant pressure (MJ/kg/℃). e_z^o is the saturation vapour pressure of air at height z (kPa), e_z is the water vapour pressure of air at height z (kPa), γ is the psychrometric constant (kPa/℃), r_c and r_a are the respective canopy and aerodynamic resistances (s/m).

Water that has not evaporated from the root zone enters the soil profile increasing its moisture content by filling the pore spaces in the matrix. It can then flow in both saturated and unsaturated conditions; whereby gravity is the main actor in the unsaturated condition with predominantly downward flow and saturated flow is governed by hydraulic pressure gradients from high to low in the horizontal direction. SWAT only simulates saturated water flow directly and assumes the water is uniformly distributed within a given layer, which eliminates the need to model unsaturated flow in the horizontal direction. Eventually the flow becomes vertical and percolates down to the capillary fringe where there is a possibility of revaporation to the vadose zone or a continuation to the groundwater systems as recharge.

The steady-state response of groundwater flow to recharge is as follows (Hooghoudt, 1940):

$$Q_{gw} = \frac{8000 \cdot K_{sat}}{L_{gw}^{\ 2}} \cdot h_{wtbl}$$

where Q_{gw} is the groundwater flow into the main channel on day I (mm H_2O), K_{sat} is the hydraulic conductivity of the aquifer (mm/day), L_{gw} is the distance from the ridge or sub-basin divide of the groundwater system to the main channel (m) and h_{wtbl} is the water table height (m). In the SWAT model, the water table height is updated daily.

The two parameters that were ultimately calibrated are HU and GW_REVAP. Heat units are defined as the total number of units required for a plant to reach maturity. Groundwater revaporation is the movement of water from the shallow aquifer to the unsaturated zone (via the capillary fringe). This is most common during dry periods when water is removed from the capillary fringe via evaporation and will diffuse upwards, replacing itself with water from the shallow aquifer. This is also possible through deep rooted plants that are able to take up water directly from an aquifer and this process becomes increasingly relevant with shallow water tables. If GW_REVAP lies closer to 0 the movement of water is restricted, however if it lies closer to 1, it will equal the ETp and varies for all HRUs.

In setting up SWAT, data from various sources had been garnered in order to reach the level of detail required for this study. The GIS files from the source partners were of 250m resolution which provided an optimal level of detail with regard to processing time and accuracy. Information from the five neighbouring meteorological stations was incorporated as well, including precipitation, temperature, humidity, wind speed and solar radiation. The five stations were from the cities of Cordoba, Marmolejo, El Carpio, Lora del Rio and Santaella.

14 landuse classes and 6 soil classes also had to be incorporated into the model as crop production is an integral part of the study and has significant influences on the total water balance of the sub-basins and certainly for individual HRUs (there were 127 in total). The DEM was used to delineate the catchment of the GCIS itself, whereby two main tributaries were identified which would ultimately drain the entire watershed. In delineation, the stream definition was set to a minimum of 1000 ha and the whole watershed is drained through one outlet in the NW edge of the catchment where these two tributaries meet. A number of reservoirs were also being tapped to supply the irrigation scheme and these three have been identified in subbasins 8, 13, 17 (see figure 5). The option to irrigate was set to “auto” at 0.16 heat units, which implied that whenever a water stress condition was reached (set to 95%) the flow of irrigation water from the reservoirs would initiate till field capacity was restored. The reservoirs total an area of 3360 Ha, and are given sufficient volume such that they do not fully drain, ensuring a constant supply of irrigated water if necessary.

Finally a monthly report of water and crop outputs was produced from January 2002 till August 2008. From here, the data must be compared with those results produced by SEBAL derived data and again recalibrated. ETact from both SWAT and SEBAL are compared and then HU (heat units) and GW_REVAP (ground water revaporation) are calibrated until the best match between SEBAL measured ETact and SWAT produced ETact is reached. With the calibrated parameters a water balance is estimated and if possible the depth to groundwater given the initial depth from the study area (if known). The idea can be carried further to use this information to derive the depth to groundwater in other ungauged areas, using remote sensing as the main (non-invasive) survey technique.

With the above data, SWAT is complete (parameterized) and can perform calculations to determine the water balance and the biomass production of the GCIS for all considered years. A comparative analysis of the findings reveals whether the results are reasonable and a check of the parameters via PEST or other methods may be used if needed. Once the parameters have been attenuated they can be updated into the SWAT model for more accurate results. All land based-data has been incorporated by this stage and the satellite component of the experiment takes precedence. Data from the RS MODIS satellite is used to calculate ET much like the SWAT model, however it uses different methods to estimate climate data. Via remote sensing the MODIS sensor uses radiances to estimate the temperature. After all the heat fluxes have been balanced along with the available moisture, SEBAL estimates the ET at a resolution of 1km. The “measured” SEBAL actual ET and the SWAT produced actual ET are compared for agreement. The most sensitive parameters (ie. HU and GW_REVAP) are then adjusted for to reproduce the SEBAL ET resulting in a calibrated model. The calibrated model is forced with a climate change prediction from which a water balance for the future is projected.

3.3.2 GCIS model

A DEM of 250m provided a good resolution of the basin while maintaining a detail level that would not take excessive amounts of computer time to process data thereafter. The shapefile provided by IFAPA was reprojected to that of the DEM (UTM 30N). The DEM itself was then used to delineate the sub-basins and the entire extent of the GCIS. Setting the stream definition to 1000 Ha created 17 sub-basins and the whole watershed was drained by a single point outlet. Reservoirs were also included in the sub-basins, however they serve to act as a delay rather than as a source of precipitation, being filled up mostly by upstream runoff rather than direct precipitation. Note however that precipitation does fall directly onto the HRUs but also into the reservoirs and whenever there was water stress from the HRU itself, the auto-irrigation schedule would activate and drain water from the reservoirs until field capacity was reached. As such the reservoirs served as an effectively unlimited source of water, having a storage volume which exceeded the demand of the respective crops in the GCIS. A detailed soil map was also required to build the model and this detail was also provided by the Spanish partners of the GCIS, while the rest of the catchment was based on the FAO soil map and finally incorporated into the current SWAT model where various soil types are defined. The slope was defined as single from one sub-basin to the next and the HRU definition was set to 0% so all the areas will be taken into account.

Fortunately, the data sets provided by our Spanish partners were virtually complete and the odd day per year from 2002-2008 that had no data was filled in by averaging the data on either side of the date in question so the weather generator never needed to be used in setting up the SWAT model. As such, precipitation, max/min temperature, solar radiation, relative humidity and wind data were all available from the weather stations situated in and around the GCIS in the towns of Santaella, Cordoba, Lora Del Rio, El Carpio and Marmolejo.

Detailed land-use maps (Corine landuse database E4C, EEA) had to be derived based on the Genil-Cabra shape file as this is a critical step in setting up SWAT. In order to do this, a lookup table was created that related the land-use to SWAT land-use classes eg. Olives, irrigated agriculture, bare lands etc. Thus the database of spatially specific crops was updated. Irrigation water was sourced from the reservoirs and they are assumed to have no seepage, such that all water will either flow downstream to the GCIS or will evaporate along the way or in situ.

Once all the input files are in place, the SWAT model is built and setup to run for daily time steps for all the years there is data (2002-2008). Following is a table of some of the assumed or default values used in setting up the model.

Table 5 – Assumed initial and default values for SWAT setup

Parameter	Value
Initial Groundwater Depth	1m
Threshold Depth for Revap	1m
Groundwater Delay	31 days
Main Reservoir Volume	$3x10^{7}$ m^3
Average Annual Release Rate (Reservoir)	0.1 m^3/s
Auto Irrigation	0.16
Auto Water stress	0.95

Aquifer information was not provided thus the thickness is unknown, nor the actual initial depth to the water table. Detailed basin geology was also not provided from IFAPA so shallow and deep aquifers were considered as one and the same. The water cycle is considered as a closed system in the GCIS such that the water balance can be calculated. Of course in reality even the GCIS is an open system as water does leave the catchment and eventually flows out to the ocean or gets evaporated on the way and this same water will not return in equal quantity in the next rain event for example.

3.3.3 Calibration

Using excel to record the model outputs, a forecast function much like: "=MAX(1800, MIN(3000,IF(OR(O2>1.1,O2<0.9), FORECAST(C2,L2:M2,F2:G2),1800)))" was also implemented. It takes a minimum of 1800 and maximum of 3000 heat units and if the result is insensitive (meaning between 0.9 and 1.1) then the minimum of 1800 is assumed. If the parameter is sensitive (meaning it occurs outside of 0.9 to 1.1) then a forced iteration takes place till the appropriate value for heat units is reached giving the resultant a best fit between the previous best model runs. From previous literature it appears that ground water revaporation and heat units are the most sensitive parameters to affect the water balance. (See graphs below for sensitivity analysis). Thus the observed actual evaporation from SEBAL was compared with the ET_{act} from the initial SWAT model parameters. Then the inputs of gw_revap and heat units were modified in succession b4 an optimal combination would result that brings the SWAT results closest to the SEBAL observations. (See appendix).

Figure 10 – Most sensitive parameters to calibrate in SWAT to match SEBAL ETact (Immerzeel, 2007)

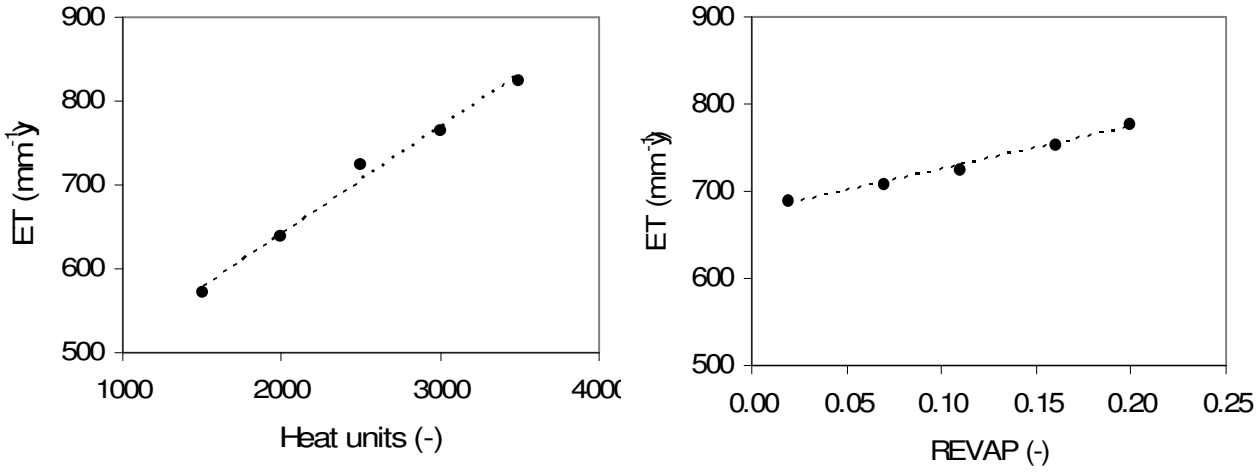

3.3.4 Climate Change Scenarios

With the climate change scenario considered, the newly optimized model was fed with the latest projections available from the IPCC as mentioned in the introduction. In this scenario for southern Spain, one can expect increased temperatures and decreased rainfall as mentioned earlier. The resulting water balance is then described in the results and discussion sections. The projections were included in the now calibrated SWAT model on a seasonal basis as that is the accuracy of the predictions, such as 2.6 degrees C increase and 6% less rainfall for December, January and February and some other variations for March, April and May etc. (See Table 1).

3.3.5 Analysis

Any water balance is difficult to produce in reality especially when considering larger scales (catchment scale for example), but also as it would assume incoming water and outgoing water at one specific instance. Theoretically, the total amount of water entering a catchment must equal whatever comes out since it is assumed to be a closed system for long time scales. Time lags vary of course depending on which aspect of the water cycle is being referred to. Surface water, rainfall, evaporation, and runoff fluxes occur on the time scale of hours, whereas the flux of groundwater and percolation for example takes place over days and weeks if not longer. Hence the overall water balance for a specific rain event cannot be known unless every drop is accounted for through natural processes and in their own time from the moment they enter the catchment to when they exit the catchment. This could be possible if there is much time between rain events and the contributions from each source (rain, soil, groundwater etc.) is clear, however in practice this is difficult to achieve despite chemical analyses and other methods to discern the sources of water.

Various time lags are considered in SWAT and antecedent conditions carry from one day to the next. This allows for a fairly good measure of the conceptual and actual flows of water as they move through the vadose zone down to the groundwater level. In order to analyse the water balance, a sum of all fluxes was made to create an average of the conditions between the years 2002-2007 for each month. Since SWAT is both a hydrological-crop production model it represents the actual physical processes very well for the entire catchment.

The water balance equation is as follows:

Precipitation + Irrigation + Revaporation = ET + Runoff + Percolation + Qlat + dS

dS – change in soil moisture

The same components are used to balance each other out in the climate change scenario.
(See figure 14 for a visual interpretation of the components which make-up the water balance).

4.1 SEBAL

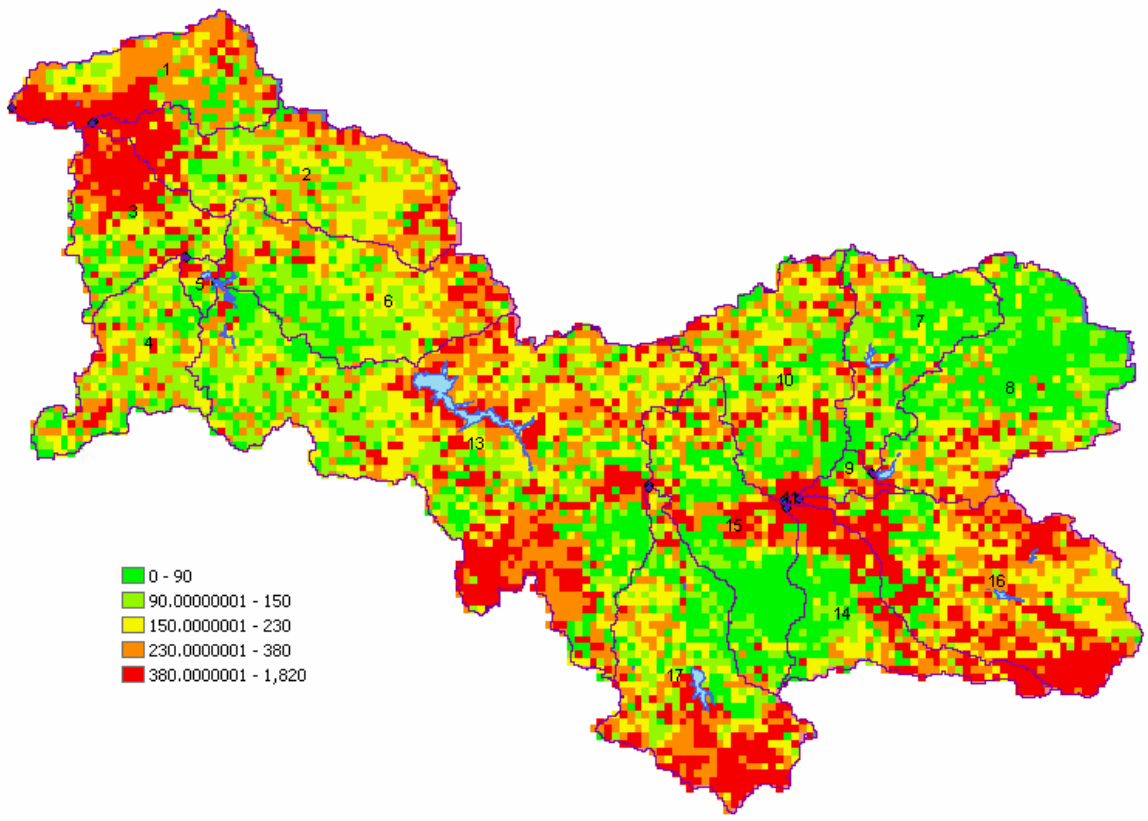

Scale – 1:800,000

Figure 11 – ETact in mm water measured by SEBAL from October 2004-September 2005

Figure 11 shows all 17 sub-basins within which are the 127 HRUs in the GCIS catchment and their associated ETacts. It shows the measured ETact through SEBAL and the resulting map has data that is separated by standard quintiles into 5 colours ranging from 0-1820 mm of actual evapotranspiration totaled for the year. It is clear the greater amounts of ETact are occurring in the GCIS itself in the NW corner (the outlet) of the catchment as well as in other convergence points of flow indicated with blue dots and of course around the reservoirs where open water is abundant. Bodies with large surface areas naturally allow for greater interaction between the water and air interfaces, thus increasing ETact. ETact varies quite considerably across the landscape despite receiving near-uniform radiation and rainfall.

4.2 SWAT

4.2.1 Calibration

Table 6 – Abridged calibration showing best match for ETact in mm (10/04-09/05)

HRU_ID	SEBAL ET (mm)	SWAT run 1	GW_REVAP 1	HU1	SWAT run 5	GW_REVAP 3	HU3
1	496.875	461.809	0.02	1800	499.681	0.072	1800
2	643.283	499.24	0.02	1800	657.916	0.269	2010
3	637.473	496.651	0.02	1800	728.899	0.221	1800
4	650.000	485.179	0.02	1800	649.783	0.209	1800
5	650.699	499.905	0.02	1800	651.435	0.179	1800
6	648.980	482.253	0.02	1800	646.547	0.259	1800
7	648.998	520.488	0.02	1800	646.133	0.300	1998
8	486.501	511.41	0.02	1800	479.578	-0.036	1866
9	496.875	497.159	0.02	1800	423.966	-0.300	1800
127	262.067	500.334	0.02	1800	405.558	-0.300	1800

(Note. - For full calibration results for all HRUs see appendix.)

Table 6 offers a glimpse of the observed SEBAL ETact vs the SWAT produced ETact. It was the fifth run of SWAT with the first four resulting from different combinations of GW_REVAP and HU values. The last column considers the sensitivity of the parameters. Only those that were outside the range of 0.9-1.1 were considered for “forecasting” to produce the calibrated values, otherwise they would be assigned the self-imposed boundary values of 1800 HU for example. Similarly for GW_REVAP – limits were established between -0.3 to 0.3. If parameter values occurred within the ranges mentioned above they spoke of values that were insensitive and thus would be unable to make a big difference to the final ETact calibration. Notice from table 6 that SWAT run 1 corresponds to HU1 and GW_REVAP 1 whilst the final optimization or calibrated model comes from SWAT run 5 corresponding to HU3 and GW_REVAP 3. The intermediate runs corresponded to various combinations of GW_REVAP and HU values before the final optimization was achieved. The forecasting technique required four previous model results for ET, before being able to calculate the fifth and final optimal parameter values that would produce the closest match between SWAT based ET and SEBAL derived ET.

As can be seen from table 6 above, the fifth run of SWAT is the closest match to the SEBAL ET for most of the HRUs. Notice that significant disparities can and may still exist between the two ET results however these reasons are alluded to in the following section.

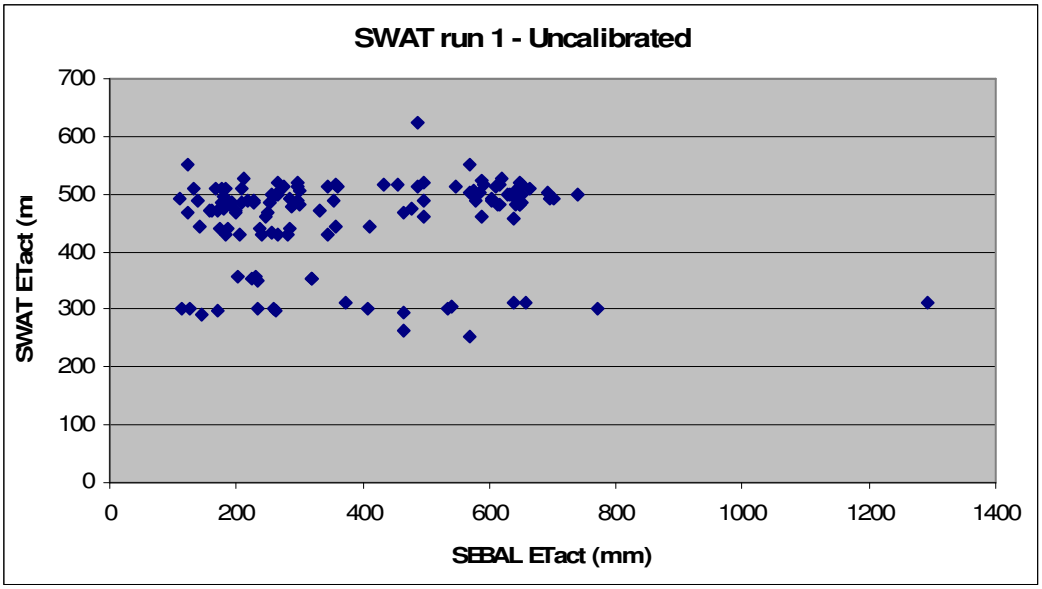

Figure 12 – Uncalibrated SWAT model showing ETact vs SEBAL Etact.

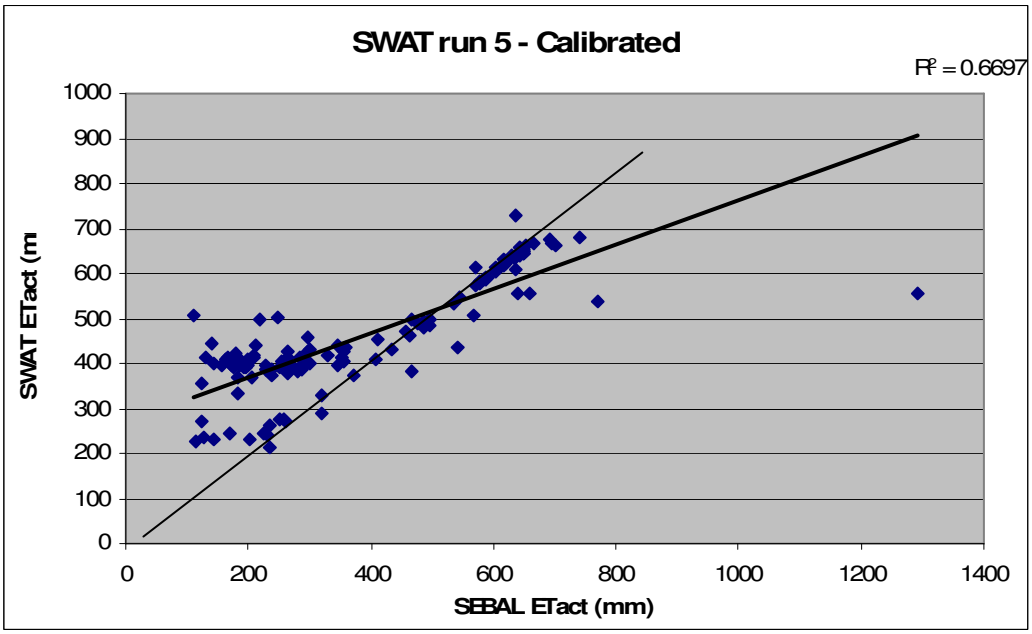

Figure 13. Calibrated SWAT model showing ETact vs SEBAL ETact.

There is an obvious and dramatic difference between the two models and in the best calibration the r^2 value stands at 0.67 (trend line shown in thicker black) which is a fairly good correlation between the ETact calculated by SWAT and observed by SEBAL. The thinner black line is drawn to show a 1:1 relationship for comparison. There are a few outliers and these can be accounted for on several levels. SEBAL records did show some unusual drop-off measurements of ET, where one day would suddenly show a 250 mm decline, and then recover just as quickly the next day to maintain the 400 mm average for example. SWAT seemed to show a consistent level of 400 mm of ET while SEBAL recorded around 200 mm (see figure 13 above). These drop-offs could occur on days when cloud cover prevented the satellite from recording an accurate and clear image of the surface or if the sensor simply failed to operate on

certain days. Another possibility is that SWAT incorporated weather data from all five weather stations and if one recalls the climate graph from figure 4 there is a slight discrepancy from regional weather and local (Santaella) weather but mostly in the summer months and in October. SEBAL has recorded data for the whole basin as well but it is much more localized within the GCIS so may agree more with data coming only from Santaella as opposed to an average of all five weather stations. Other differences could be derived from the fundamental differences in how the two models calculate ET, however this is why there is a calibration process - to enable one set of data to relate to the other and vice-versa and to fill in the blanks where necessary such as in previously ungauged basins or PUBs.

4.2.2 Water balance

Since 2002 at least, there seems to be a mis-match in natural water schedule demands in the catchment, hence the need for an irrigation scheme is obvious. With the water stresses increasing over time the need for more irrigation is necessary in order for the region and its crops to be sustained into the future. There will be additional tapping into the reservoirs and aquifers as well and hopefully their reserves will be sufficient to compensate for the lack of surface water available within the catchment itself. Whenever water starts to be drawn from aquifers however it is only sustainable if it is being equally sufficiently recharged, however recharge in this basin is already fairly limited and according to future predictions will only get increasingly stressed.

Table 7 – Average Monthly Water Balance of the GCIS (2002-2007)

(mm)		in			out				
	month	Prec	Irr	Revap	ETact	Runoff	Perc	Qlat	dS
Jan	1	34.5	0.0	0.1	-17.0	-1.7	-7.2	-1.6	-7.1
Feb	2	52.4	0.0	0.1	-24.9	-3.9	-9.7	-1.5	-12.5
Mar	3	55.1	0.0	0.1	-38.2	-5.7	-5.0	-1.8	-4.5
Apr	4	37.7	0.2	0.2	-48.6	-2.1	-1.2	-1.4	15.2
May	5	49.9	20.0	0.4	-74.8	-7.2	-0.5	-1.1	13.3
Jun	6	37.9	24.1	1.0	-93.2	-1.7	-0.5	-0.6	33.0
Jul	7	12.1	6.1	1.5	-48.9	-0.2	0.0	-0.4	29.7
Aug	8	4.2	0.2	1.4	-14.1	0.0	0.0	-0.2	8.5
Sep	9	15.4	0.3	1.0	-6.5	-0.2	0.0	-0.3	-9.7
Oct	10	43.4	1.3	0.5	-10.9	-1.7	0.0	-1.4	-31.1
Nov	11	48.8	0.3	0.2	-11.1	-1.4	-1.3	-1.7	-33.7
Dec	12	72.5	0.0	0.1	-16.3	-4.8	-6.8	-2.3	-42.4
Total		**463.9**	**52.5**	**6.6**	**-404.7**	**-30.7**	**-32.3**	**-14.2**	**-41.2**

Total average annual precipitation between January 2002 and December 2007 is 463.9mm of which 404.7mm is lost through evaporation. When considering the other terms in the balance it is clearly vital that irrigation be applied lest the soil be dried out and would ultimately be unsuitable for farming. Green shows the incoming water and orange shows the outgoing water in the balance. dS is the change in storage and ultimately relates to the change in soil moisture. Within catchments water is generally an open system but no leakages are

considered and in order to close the balance the dS term is introduced which is the change in soil moisture or storage.

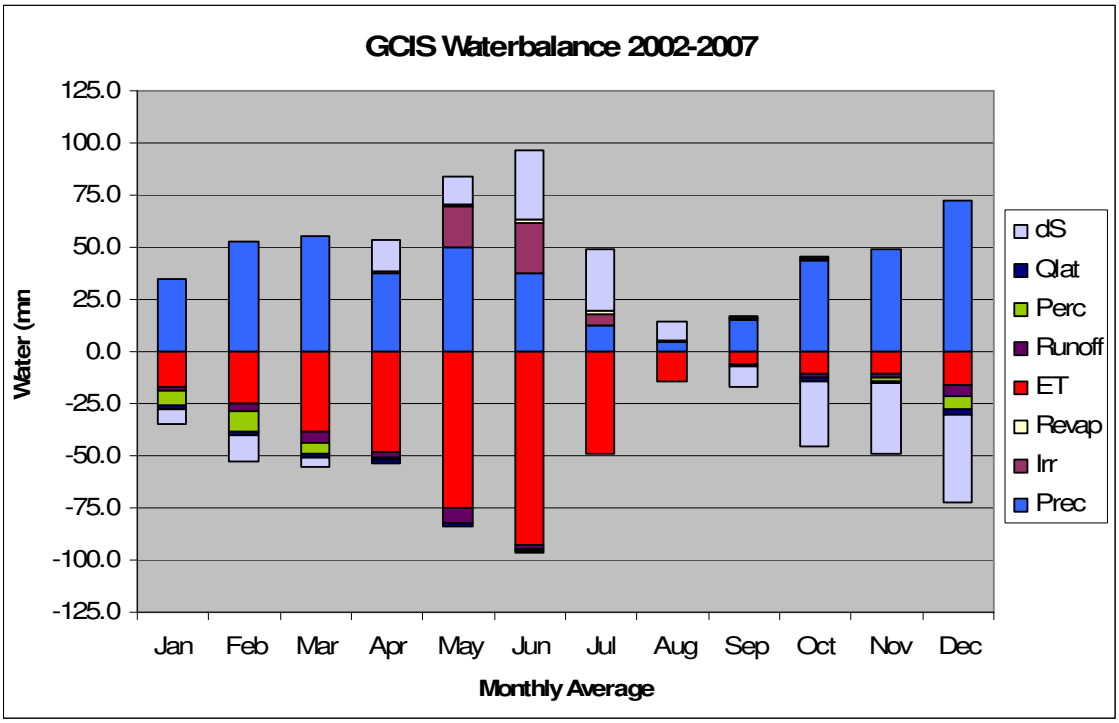

Figure 14 – GCIS water balance with all sources and sinks

From the water balance (see Table 6 & Fig.14) it is clear to see that this is a water-limited environment such that the majority of incoming water is lost through evaporation fairly quickly. August is easily the driest month with no runoff and no aquifer recharge, which implies the soil is very dry as whatever water is available is being immediately soaked into the thirsty soil. This process started in July as percolation had already stopped by this point and soil moisture is certainly very low due to consecutive months of negative storage values (dS). The other extreme sees February and March as the wettest months with relatively higher percolation and runoff values as they are the result of consecutive months of positive soil moisture storage.

From Fig.14, where the first main water balance is produced, there are some critical points to mention. While 85% of precipitation in this region is lost through evaporation, the other components are an order of 10 lower in amounts of water for the entire basin. Yet their importance cannot be overstated, as it is in these lower order components where the true balancing act takes place. Irrigation water could just as easily be lost as runoff and lateral flow, however Qlat does occur within the root zone and is of benefit to the plants and animals growing and living off the soil respectively. When considering recharge the time scale changes considerably and in this case a 31-day lag was assumed. This explains why percolation levels peak at least after one month has passed as it takes time and various pathways (fingered flow for example) for water to infiltrate the soil, not be revaporated or transpired by plants, or held within the soil before it is able to contribute to the water table (which was initially assumed to occur at 1m depth). This is clearly demonstrated as in both the normal and climate change

scenarios, peak percolation or recharge occurred in February whilst peak rainfall occurred in December (see figure 21).

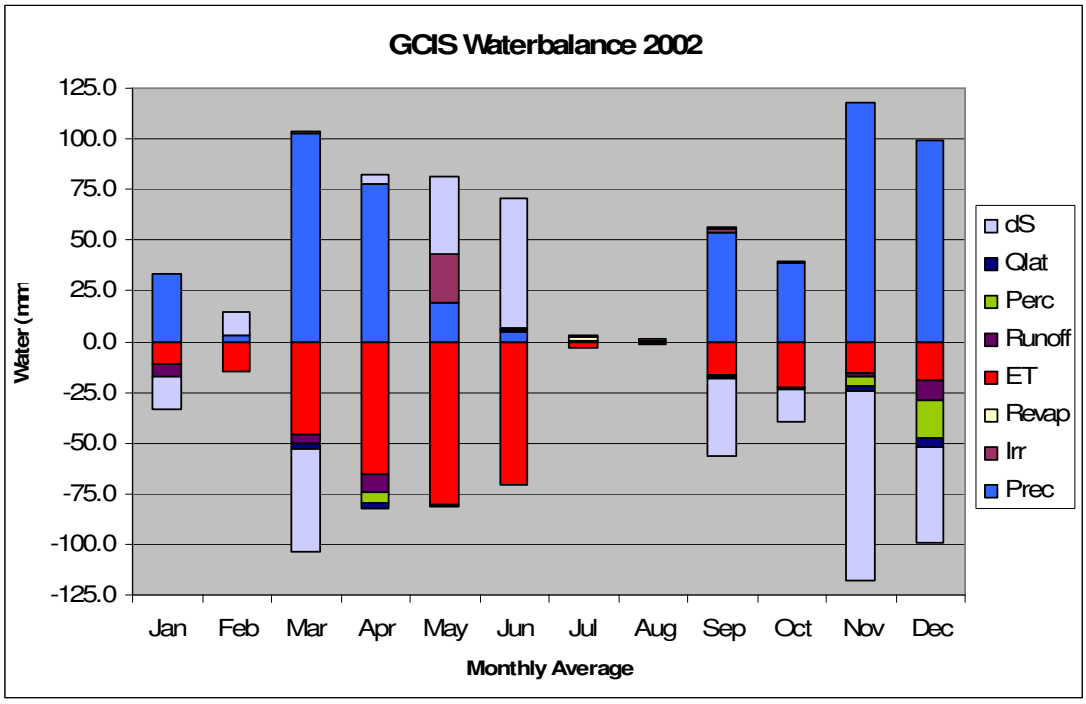

Figure 15 – GCIS Water balance for 2002 (most precipitation)

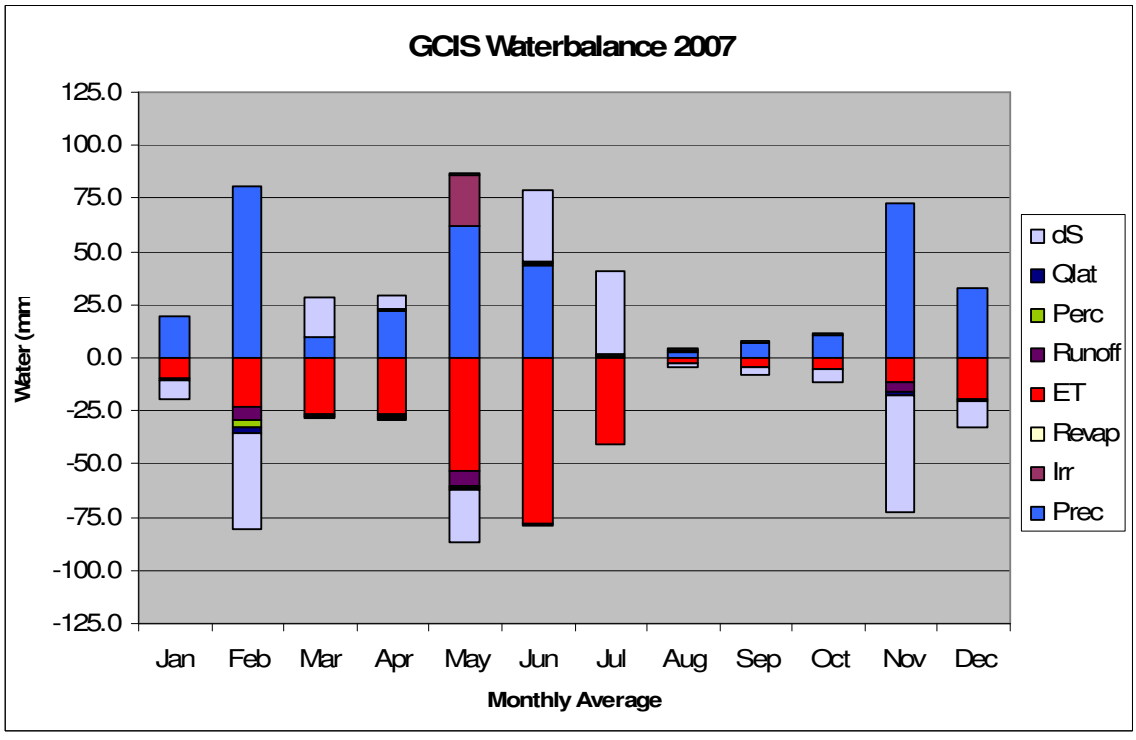

Figure 16. – GCIS Water balance for 2007 (least precipitation)

For the years of investigation a summation of the ETact is produced per land-use to see which crops produce the greatest amount of evapotranspired water for each month of the year in absolute terms (see figure.15 below). Volumes are greatest in the summer months when

water is most available and there is significant energy available to evaporate it and the plants are approaching harvest time. Immediately after harvest the crops show very little evaporation as they are least active and fortunately there is less water available in the system anyway. After the lowest ETact experienced annually in September, there is a gradual build-up again of photosynthetic activity when the planting and growing season commences in the autumn and winter respectively but doesn't gain much momentum until the spring when most crop plants reach maturity. It is curious to note that bare soil loses as much water for much of the year through direct evaporation as many other crops, except that of course the plants are transpiring water as well for crop production and the general health of the region's ecosystem.

It is also interesting to note the extreme years of 2002 and 2007 being the wettest and driest in terms of rainfall respectively. That is not to say that these years were actually the wettest or driest overall. For example 2004-2005 shows a period of low rainfall and very high ETact so could translate to a drier period ultimately than just 2007's low rainfall and subsequent lower ETact. Having said that 2002 does have the highest rainfall and relatively lower ET so should ultimately be the wettest year in the study period. Regardless of the year, the seasonal patterns are consistent - that is dry summers and wetter winter and spring seasons.

While absolute volumes are indicative of the amount of water in the system lost through various landuses it still doesn't tell us which crops truly are the biggest contributors to evapotranspiration in the GCIS. See figure 17 for relative evaporative demand of each crop for the same time period.

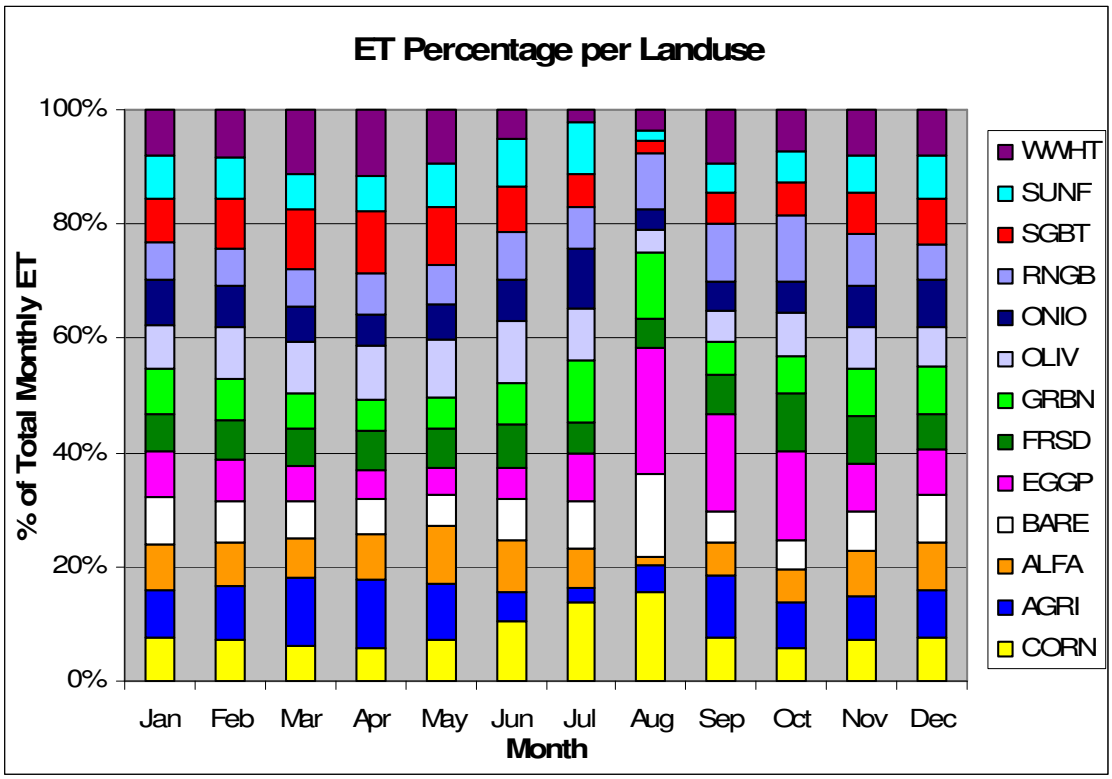

Figure 17 – Relative quantities of ETact for the 13 land-uses.

From November till February the proportions are fairly stable and nearly equal for all land-uses. Moving into the mature phase of plant growth in the spring, various crops take over their share of ETact whilst others lose out. The various cycles can be easily observed through this graph as different crops emerge as the dominant players in the water balance. For example sugarbeet, winter wheat, olives and irrigated agriculture seem to dominate from March-May, while suddenly in the summer months corn and later eggplant are predominant consumers of water (not to mention the August contribution to ETact from bare soil).

These results still do not tell us which are the more productive crops or lands. That is determinable by yield per hectare of land (see figures 18 and 19). This graph plots the sum of the crop yield per month with water contributions from both rainfall and irrigation.

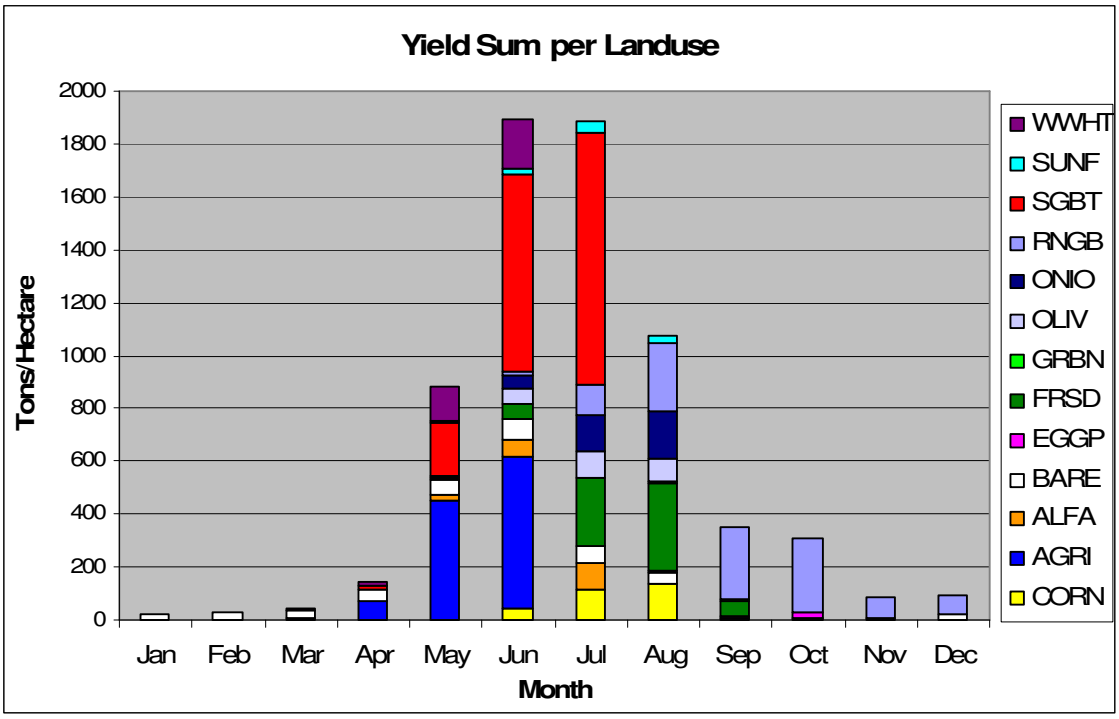

Figure 18 – Sum from 2002-2007 of monthly yields for various crops in tons per hectare.

From the initial landcover types, olives took the greatest amount of land accounting for 43% (see table 3) of the watershed area, however they appear to have a lower yield, totaling just 246 tons/ha. This is quite unlike sugarbeet and irrigated agriculture which share yields greater than 1000 tons/ha yet only make up less than 1% of the watershed area of the GCIS.

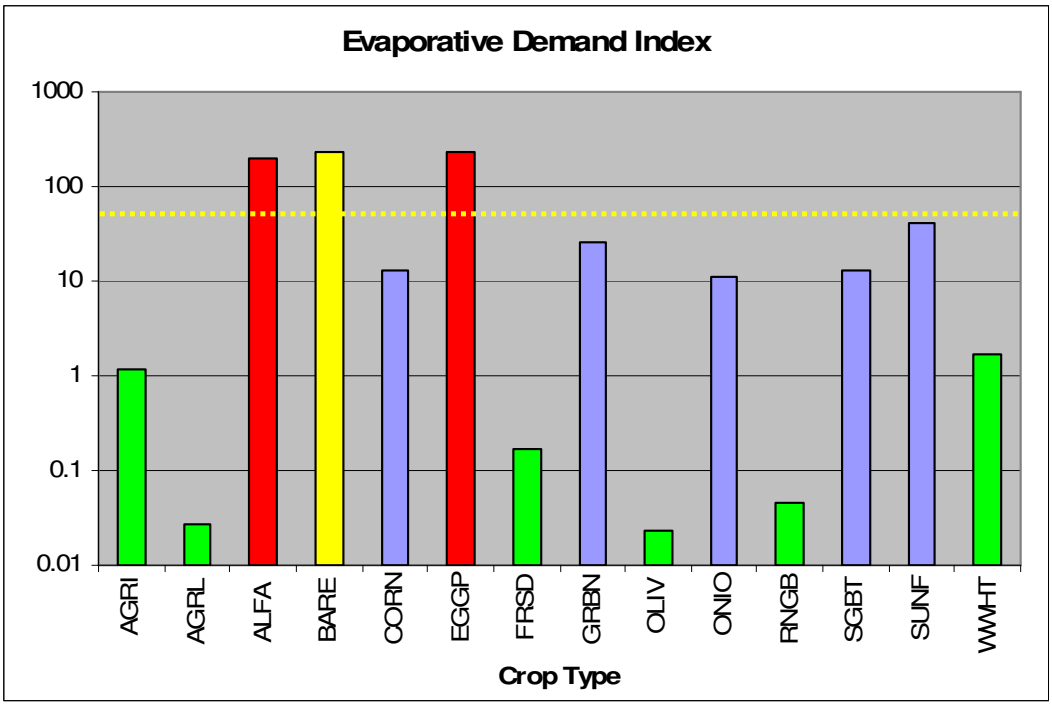

Figure 19 – Evaporative Demand Index (EDI) of crops in the GCIS

The above graph (figure 19) was created by dividing the annual sum of ETact by the sum of the area in km² in which the crop grows to produce an evaporative demand index. This allows for comparison of the amount of water evapotranspired by each of these crops during the course of an annual cycle. Since the evaporative demand per crop is very different, a logarithmic scale was employed for practical purposes. The yellow line indicates the average level. Bare soil is indicated in yellow and columns that approach a similar level in EDI show just how closely various crops mimic the effect of no cover on that specific HRU's water balance. The blue columns indicate crops that are at a moderate level of EDI, whilst green columns highlight cover/crop types that are very sparing in water consumption and red indicates relatively high EDI. Alfalfa and eggplant appear to be two of the thirstiest crops grown in the catchment whilst generic agriculture, olives and range brush consume the least amount of water per km² of each specific crop.

The crop that produced the highest ETact as a percentage of the area it covers is eggplant followed by bare soil as a close second. Whilst eggplant was somewhat of a surprise bare soil seems reasonable, as without any cover the soil is completely exposed to the elements and the sun can easily warm the ground while the wind is met with no resistance. This allows for a continuous moisture gradient to exist between the moist soil interface and the dryer and warmer air above it causing more rapid water evaporation off the surface. However one may consider the possibility of the top crust drying out quickly forming a non-permeable layer preventing additional drying below.

Plants with a lower leaf area index (LAI) will naturally have a lesser coverage of the ground thus are less able to shield the soil surface from direct insolation. After further

investigation it therefore accounts for the surprise that in the case of eggplant, which has one of the lowest LAI's amongst all the crops (only second to bare soil), there is more evaporation from the surface as well as the added transpiration the plant requires through the year to survive resulting in it being the crop with the highest evaporative demand. Fortunately and probably not surprisingly, it covers just 25 hectares in the entire catchment (nearly 0%) of the total area along with bare soil in fact at also just 25 hectares. This does not mean that eggplant itself is the thirstiest of the lot, because that is determined purely by transpiration alone, which was not isolated in this investigation since this study is based in reality where both evaporation and transpiration are constantly active.

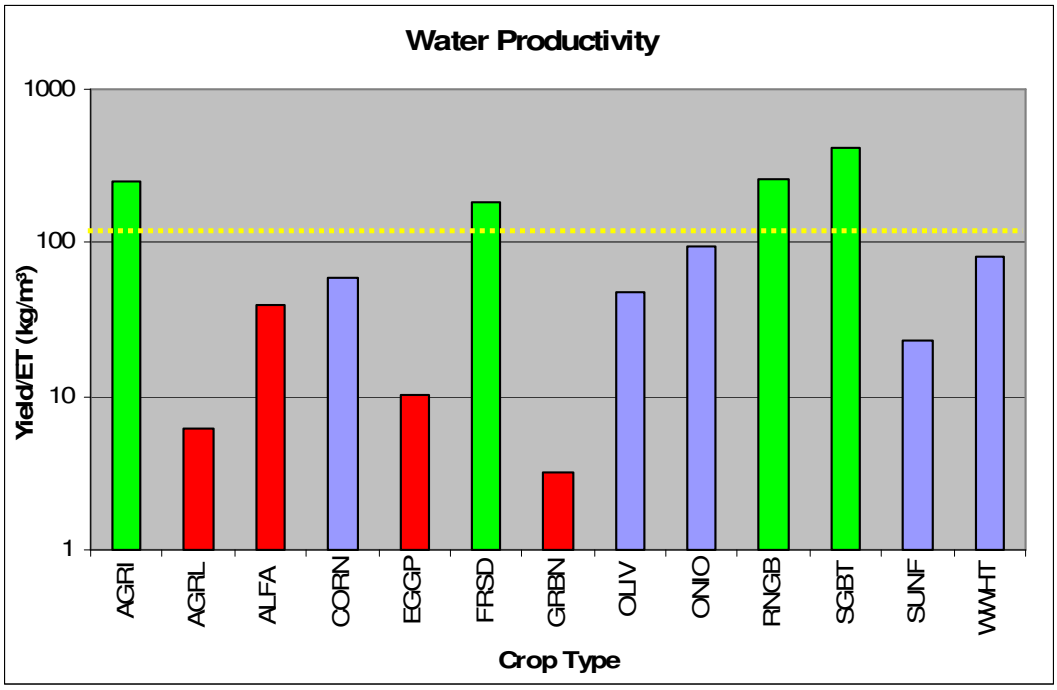

Figure 20 – Water Productivity of the various crop-types

Figure 19 and 20 are rather telling as they highlight some fundamental management concerns regarding the type of crop grown, their productivity and water usage efficiency. Figure 20 was produced from dividing the annual yield sum (tons/ha) by the ETact resulting from that same year for the corresponding crop. It is interesting to note that the crops that were considered thirsty are also not water productive such as the case with alfalfa and eggplant. The only real surprise was generic agriculture (rain-fed) which shows low water productivity but it is also one of the least demanding landuses in the basin so it is not detrimental to the overall basin especially when one considers it is the dominant land-use. The yellow line in this graph is the mean crop productivity at 105 kg yield per m^3 of evapotranspired water. Clearly the green columns indicate high productivity, consistent with figure 18, showing sugarbeet as the crop that is the most efficient water consumer.

4.2.3 Climate Change Scenario

Table 8 – Average Monthly Water Balance of the GCIS with Climate Change 2089+

(mm)		in			out				
	month	Prec	Irr	Revap	ETact	Runoff	Perc	Qlat	dS
Jan	1	32.4	0.0	0.1	-18.2	-1.4	-4.2	-1.4	-7.4
Feb	2	49.2	0.1	0.1	-27.8	-2.9	-7.2	-1.3	-10.1
Mar	3	46.3	0.1	0.2	-45.7	-2.7	-1.1	-1.4	4.3
Apr	4	31.7	12.8	0.3	-59.5	-0.8	0.0	-1.0	16.6
May	5	41.9	14.1	0.7	-80.7	-5.2	-0.4	-0.8	30.5
Jun	6	28.8	3.7	1.3	-59.8	-0.1	0.0	-0.4	26.5
Jul	7	9.2	0.2	1.6	-16.7	0.0	0.0	-0.2	5.9
Aug	8	3.2	0.1	1.4	-3.2	0.0	0.0	-0.1	-1.5
Sep	9	13.6	0.1	0.9	-4.7	-0.1	0.0	-0.2	-9.6
Oct	10	38.2	0.5	0.5	-9.2	-0.9	0.0	-1.2	-27.9
Nov	11	42.9	0.0	0.2	-10.7	-0.8	-0.2	-1.4	-30.1
Dec	12	68.2	0.0	0.1	-16.7	-3.2	-4.0	-2.0	-42.4
Total		**405.6**	**31.8**	**7.5**	**-352.7**	**-18.1**	**-17.2**	**-11.5**	**-45.3**

With the IPCC's projection applied for southern Spain, the above water balance is the result. Total annual averaged precipitation is down to 405.6mm yet ETact has decreased to 352.7mm. See the graph below (Fig.21) for a better visual representation of the above results.

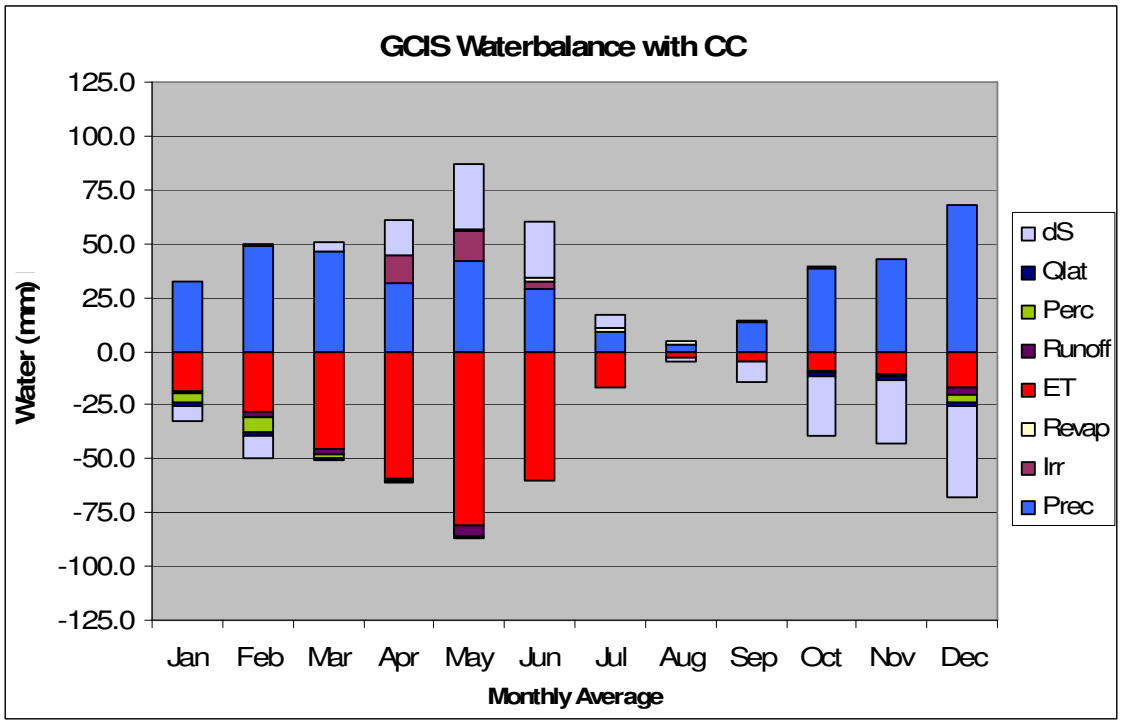

Figure 21 – GCIS water balance after climate change projection for 2089+.

With regard to the number of months where no ground water recharge was occurring, this is an expected result. It is curious to note however that the change in soil storage (dS) has increased slightly by 4mm, which means slightly more moisture is held in the soil itself and not

in the aquifer below. This may not be a significant amount and could just as easily be cast as error propagations through the model, however the climate change scenario maintained ceterus paribus besides temperature and precipitation so the model itself is consistent and its results are repeatable. This means more processes are occurring in the shallow subsurface system or the vadose zone. There is greater interaction in this layer and very little is happening below the capillary fringe as can be shown by the number of dry months. In the normal scenario, July through October saw no percolation, that is 4 months of no recharge in the aquifer. In the climate change scenario, nearly 7 months are without recharge from April till November. This gives very little room for recharge to take place in the wet season and hopefully those contributions are intense enough to replenish the aquifers but this seems less and less likely.

After the climate change variables were added to the model a host of new results came through describing the GCIS. Since the projections expected less rainfall and more heat the water balance had indeed been altered significantly. An increase in ETact was expected due to the new conditions, however it decreased due to the available water which had also declined since there was less precipitation as expected. ETp did increase however, so the model was not erroneous in this regard. The reservoirs were set at a high volume and were to serve as the source of irrigation in the system. Whenever there's a water stress the irrigation systems activate and this should also be reflected by increased irrigation, however that number also declined. One possibility is that the reservoirs have tapped out so ETact actually goes down along with irrigation because the reservoirs may be dry already and irrigation water supply has been lost. (Note. Reservoir capacity was high, but with less water available they will not fill fully).

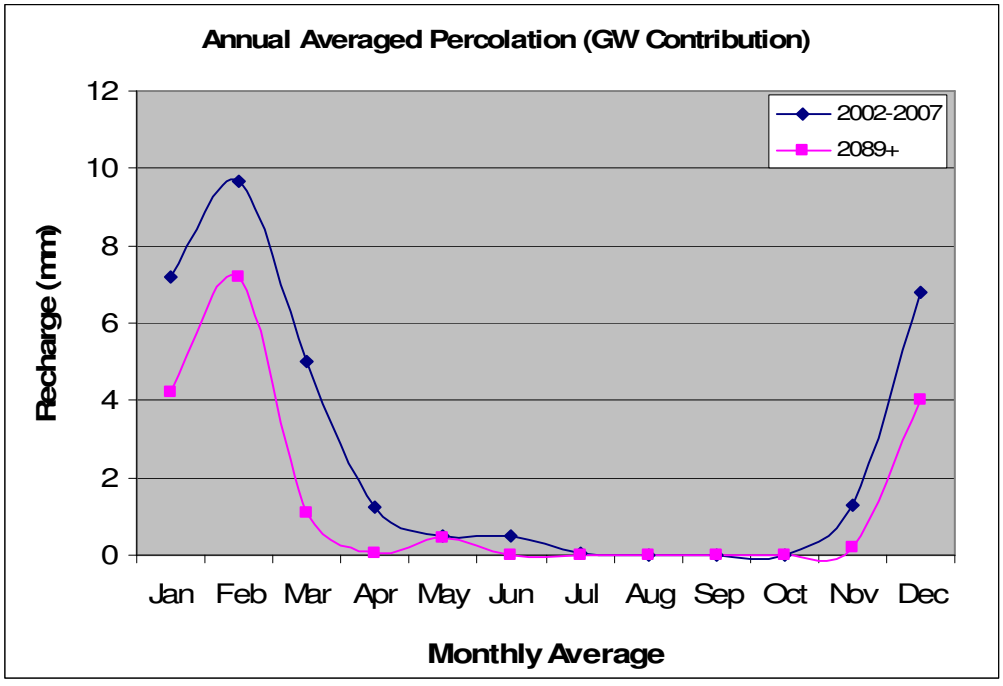

Figure 22 – Average annual groundwater contribution through percolation

The blue line indicates the amount of annual monthly percolation in the GCIS averaged for the years 2002-2007. It is clear that the summer months are the times when groundwater levels are lower since there is no added contribution to the water table and the opposite is true

for the winter months when precipitation is highest and evaporation is at its lowest. The pink line shows the same information however with the climate change scenario included. There is half as much percolation occurring in this case and the entire water balance appears to have shifted one month earlier (see figs. 14 & 21). The available water peaks in June in the original scenario; however with climate change, peak water occurs in May and will certainly have impacts on the growing season and irrigation/crop schedules. It is also clear to see the number of months when no recharge is taking place. In the original scenario 4 consecutive summer months see no percolation; whilst after induced climate change, 7 months are without percolation, indicating a possible and eventual depletion of the ground water aquifers.

Table 9 – Climate Change comparison of main components in the GCIS water balance

Annual Average (mm)	2002-2007	2089-2099	% Change
Precipitation	464	406	**-12.5**
Evapotranspiration Act.	405	353	**-12.8**
Evapotranspiration Pot.	1203	1323	**+10.0**
Groundwater Recharge	32	17	**-46.9**

While precipitation has decreased by 12.5% evapotranspiration also seemed to follow suit with a similar change of 12.8%. This may seem unusual as an increase was expected, however as mentioned earlier, ETp (potential ET) did in fact increase by 10%. The reason therefore for less ETact was most likely due to already limited water availability. However the greatest change after inducing a climate change scenario onto the GCIS was the groundwater recharge at nearly 47% less. This has huge implications for the future of the basin and implies that the planners can never tap into groundwater for more supplies as the aquifer is already significantly decreasing in recharge without any water being drawn for agriculture.

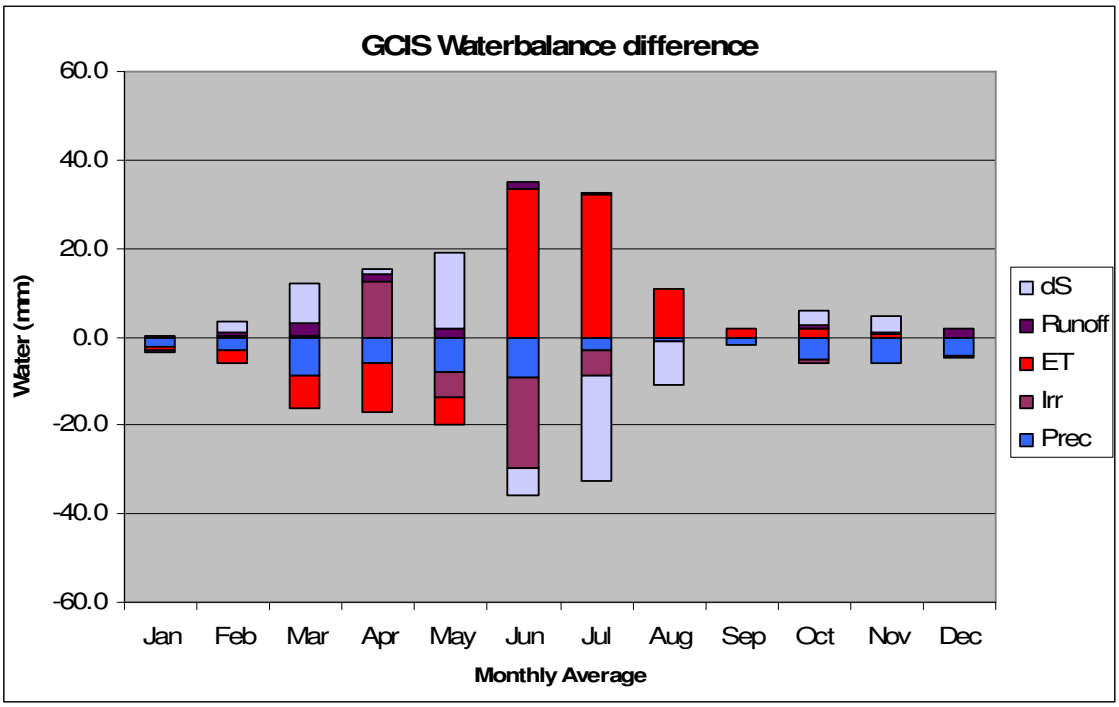

Figure 23 – Difference in water balances between current and future climates in the GCIS

5 Conclusion

The research performed in this investigation strived to discover the following:

1) If it was possible to calibrate a model on ET and the efficacy of using remote sensing on previously ungauged basins;
2) To establish the water balance of the Genil-Cabra Irrigation Scheme's watershed and assess the region's crop production and ground water resources;
3) The effects of climate change on the water balance and future implications

From the techniques discovered in the literature review and from those implemented here, it is safe to say that it is indeed possible to calibrate a hydrologic-crop production model on ET alone. In this investigation, SWAT parameters of ground water revaporation and heat units were calibrated on ET derived from SEBAL measurements. A correlation of 0.67 was established for the r^2 value for the actual evapotranspiration as calculated from SWAT and derived from SEBAL (see figure 13). This demonstrates a strong enough correlation to calibrate other models or other model parameters with SEBAL based ET to produce a more representative water balance especially in other areas where data is scarce or in PUBs.

Once the water balance was produced (see figures 14-16) one could then see the various components and the significance of their contributions to the overall watershed. The GCIS water balance is clearly shown in table 7 where gains and losses are evaluated in the watershed. The analysis of the resultant crop production showed how a water stressed region should allocate land and grow select crops to optimize water efficiency and landuse. Certain crops were identified to be thirstier than others for example while others were favourably suited for cultivation in the water-limited catchment. This analysis revealed that plots which grew eggplant, alfalfa or were simply bare soil had the highest ETact. It was also discovered that sugarbeet, range brush, forest and irrigated agriculture were the most water productive, with relatively high yields per volume of water consumed. It can also be established that the irrigation system is needed in the Genil-Cabra basin to mitigate the uneven temporal distribution of southern Spain's rain for sustained crop growth.

This investigation had initially strived to estimate groundwater levels without the need for drilling boreholes. In the process it became increasingly clear that not all the required data from IFAPA would be available or simply does not exist. It seems unlikely, yet no groundwater information was on hand. While absolute values were not possible to arrive at, due to the need for initial water table heights, relative changes in the basin can and were supposed. Common sense would suffice to say that ground water levels would be higher during the rainy season and lower in the dry season and this simply translates to higher table conditions in the winter and lower levels in the summer. The extent to which these fluctuations occur can however be discovered through this study, which was previously unknown. From figure 22 one can see a near 10mm contribution to the water table for the month of February and from table 14 a 33 mm

contribution across the entire basin is evident annually. From table 3, the weighted average of the soil depth for the whole basin (7214 km²) is calculated as 109.5 cm. In constructing the SWAT model, an assumption of 1m depth was made which is reasonable if there is bedrock below. Adding the water balance to this information and the subsequent climate change scenario, one can practically detect the fluctuations of a very thin water table indeed.

Since the catchment is large enough to have different water balances per sub-basin and even per HRU, various water balances can and have been drawn for each. Furthermore one cannot assume that the productivity of the crop is due to the inherent properties of the crop alone but also due to specific combinations like soil type and environmental conditions that allow it to thrive or not. However it has been illustrated that given the local conditions in this basin certain crops do appear more suited to higher yields with limited water than others. A comprehensive average for all the years in this study was made to give an overall water balance for each month. Still one can compare the predominant landuses and their effects on the catchment's water balance by considering the ETact from figures 14 and 21.

Figure 18 shows the EDI of the various crop types and essentially determines which crops should or should not be grown in an already water stressed environment. It seems in general the Spaniards indeed optimized the use of their lands, since the majority of the land in the catchment is used by the least demanding crops in terms of water consumption. Earlier it was found that olives have the lowest EDI and appropriately they cover 43.2% of the catchment. Generic agricultural land is second in EDI and covers 32.3% of the watershed. Third in line is range brush followed by deciduous forest and they cover 18.6% and 4.4% of the catchment area respectively. In fact the choice of crops grown here and their respective field sizes seem directly proportional to their evaporative demand derived through the model results and these findings continue to be in agreement from irrigated agriculture down to sunflowers crops and all types in between. Therefore it seems IFAPA and all governing bodies considered within the GCIS really have optimized their agricultural production whilst minimizing water consumption.

The climate change scenario produced some interesting results and invariably agreed with the projections the IPCC had suspected for the end of the 21st century. The simulation revealed some clear results (see table 9 regarding the magnitude of change expected by the end of the century and figure 23). The water balance had shifted its volumes by an entire month, such that peak water was occurring in May instead of June – the summer months in general saw the greatest differences for the past few years when compared with the end of this century. The average annual response in precipitation was indeed very similar to the IPCC's seasonal projection. The IPCC expected a 12% reduction in rainfall while the SWAT model calculated 12.5% less rain. The 3.5 degrees C warming led to a 10% increase in ETp. The combination of the two new projected climate inputs into the calibrated SWAT model produced a 47% reduction in groundwater recharge. The significance of this statistic alludes to careful management of the GCIS – no aquifers ought to be tapped to sustain the region's agriculture or else recharge will cease altogether, the aquifers may dry up, leaving the GCIS at risk.

6 Evaluation and Recommendation

Having researched the area extensively without having had the opportunity to physically go to the Guadalquivir basin and see the GCIS, one can still be relatively confident in the investigation's findings. Data from IFAPA was more than sufficient to produce a robust SWAT model with various years of data from 2002 to 2008. Having this recent set of data to work with brings forth a temporally relevant body of figures from which to make the model. Yet, it would have been even more illuminating to have data extending many more years in time to get a true sense of the system. However it is worth remembering that the part of Guadalquivir basin as it has been defined in this investigation is not a natural system, since the flow of water is controlled through the Genil-Cabra Irrigation Scheme. It is unlike a natural river system whereby the regime is evolving over a century and having discharge data is indeed relevant to predict the next flood for example. Here various gauges are constantly monitoring climatic variables which are useful for agricultural production and planning.

SWAT and SEBAL were used in conjunction in this study and the dual approach of satellite remote sensing with ground based instruments is one of the most comprehensive ways to approach a good understanding of any basin. Data can thus be verified and calibrated against the other to produce better parameters or to substitute for data that could not be produced by one method but is able to be recorded by the other method. There are various advantages to using a dual approach and its likely that forcing a model with other climatic factors besides ET may produce equally relevant results. Of course the biggest limitation in this study was alluded to earlier and that is the lack of groundtruthing. While the available data used comes from ground-based measurements such as soil surveys, weather station data etc., other hydrologic considerations were assumed as discussed previously. Groundwater measurements were not available and this is necessary to predict the height of the water table presently and after a climate change scenario is induced. Well data would also have been very useful, and no borehole was drilled in the catchment for the purposes of this investigation; therefore soil profile information, hydraulic parameters, etc. were not verifiable.

Since any model can only be as good as its input data, that is another area which could be improved on. Initially a DEM of 90m was to be used but this would have slowed down processing time significantly. Increasing the resolution would certainly have given more detailed information and perhaps more accurate data per pixel. The MODIS images however which SEBAL is based on are of a coarser resolution, so 250m as was used here would be a closer match for comparative model purposes. Had several satellite images been used with SEBAL for the same period and acquired in a similar manner, then a greater level of confidence could have been applied here as well, perhaps this is something to consider for a future investigation. Especially since satellite technology continues to improve with next generation sensors with better resolution and increasingly complex filters, it will only be a matter of time when the exhaustive ground-truthing methods such as lysimetry for ET may be less relevant especially for

catchment scale investigations. This does not imply ground-truthing itself is less relevant, on the contrary, as it is still necessary for validation

On a side note, it would be curious to know on what grounds the Spanish planners chose to allocate the sizes of their fields and to which crops exactly, as I doubt they used exactly the same method as I had invented here with regard to EDI. Also it would be curious to know from an economic standpoint, what the price of the produce is on the market and whether this equates similarly per unit of mass and if the thirstier crops are indeed more expensive or not.

With regard to climate change scenarios - there are many projections and models that can be used to generate a variety of results, yet the A1B scenario was recommended as one of the primary models for investigative purposes so it was used in kind here.

7 References

IPCC 4th Assessment – Working Group 1, Climate Change 2007 “The Physical Science Basis” Chapter 11, Regional Climate Projections.

Immerzeel, W. W. and P. Droogers - Calibration of a distributed hydrological model based on satellite evapotranspiration. Journal of Hydrology, 2007, vol. 349(3-4), pp 411-424.

Immerzeel W. W., Gaur A., Zwart S. J - Integrating remote sensing and a process-based hydrological model to evaluate water use and productivity in a south Indian catchment. Agricultural water management, 2008, vol. 95, no.1, pp. 11-24.

C.Santos, I.J. Lorite, M.Tasumi, R.G. Allen, E. Fereres - Integrating satellite-based evapotranspiration with simulation models for irrigation management at the scheme level, Irrigation Science, 2007, Volume 26, no.3, pp 277-288

Spain map – http://www.maps-for-free.com and (www.wikipedia.com)

Guadalquivir River Image – W. Blomquist, C. Giansante, A. Bhat, K. Kemper, Institutional and Policy Analysis of River Basin Management, World Bank Policy Research Working Paper 3526, 2005, pp. 4

Food and Agriculture Organisation, FAO Soil Map (1995)

W. G. M. Bastiaanssen, M. Menentia, R. A. Feddes and A. A. M. Holtslag - A remote sensing surface energy balance algorithm for land (SEBAL), Journal of Hydrology, Vols. 212-213, 1998, pp 198-212.

Penman, H.L. - Evaporation: An Introductory Survey. Netherlands J. Agric. Sci. 1:9-29, 87-97,151-153. (1956).

C.W. Thornthwaite - An Approach Toward a Rational Classification of Climate. *Geographical Review* 38: 55-94. (1948).

Sensitivity Analyses – Highest gradients are most sensitive

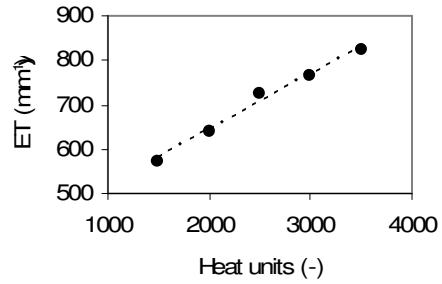

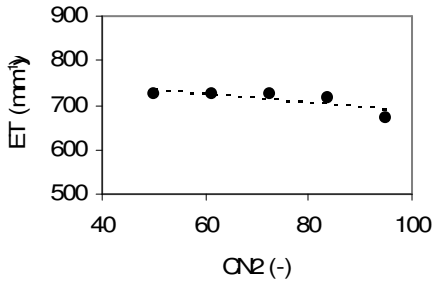

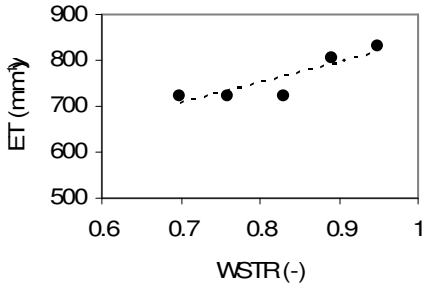

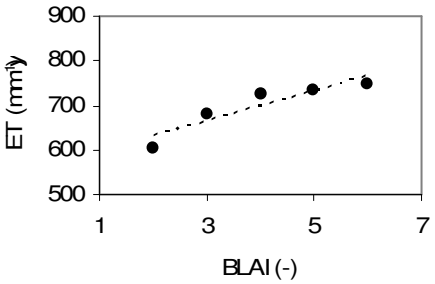

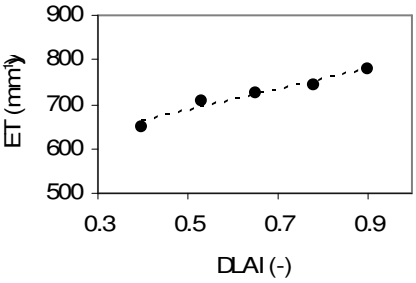

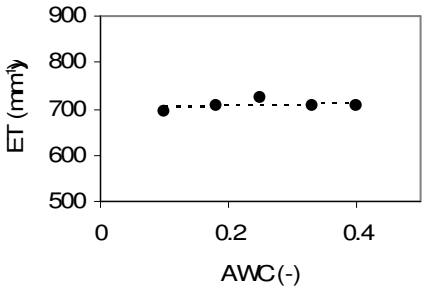

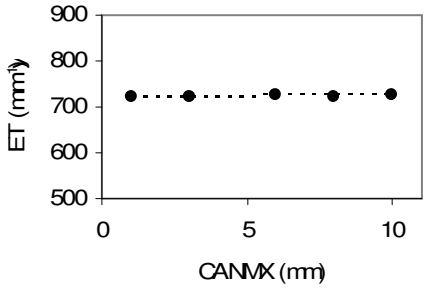

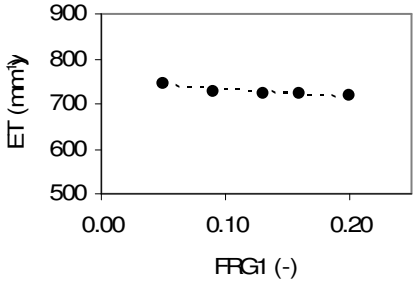

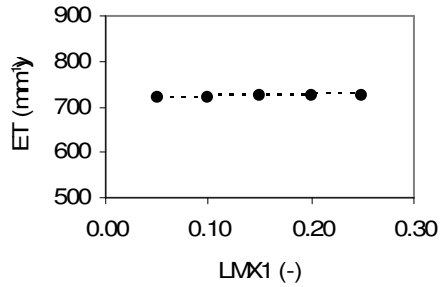

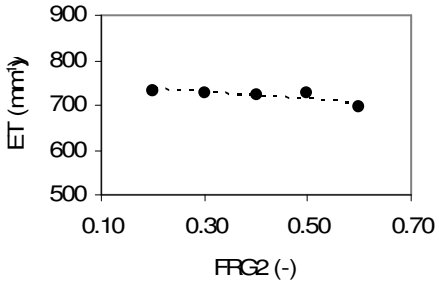

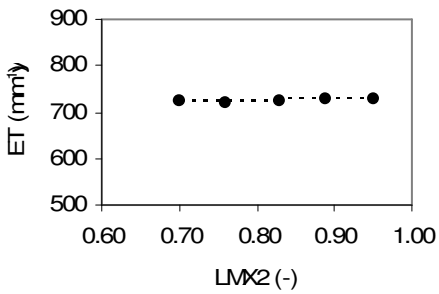

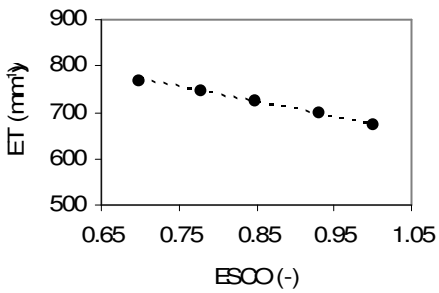

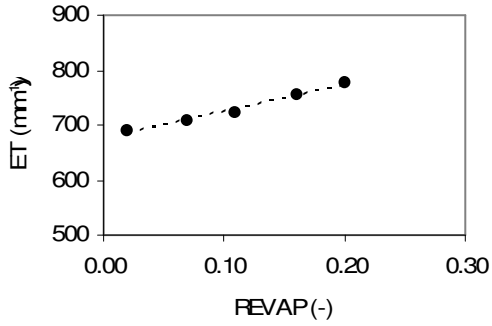

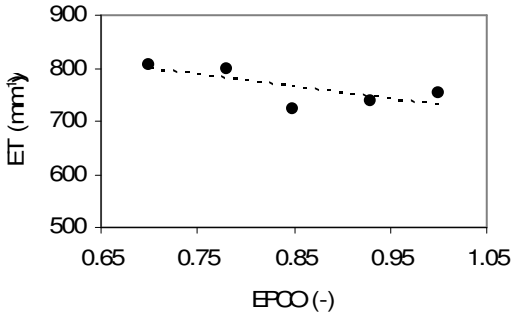

Full Calibration – SWAT run 5 based on Revap 3 and HU 3, closest match with SEBAL ET (mm) Actual Evapotranspiration per HRU

HRU ID	SEBAL ET	SWAT run 1	SWAT run 2	SWAT run 3	SWAT run 4	SWAT run 5	REVA 1	REVA 2	REVA 3	HU1	HU2	HU3	Sensit.
1	496.9	461.81	582.92	499.681	523.485	499.681	0.02	0.2	0.072	1800	3000	1800	1.047638
2	643.3	499.24	603.43	629.46	708.294	657.916	0.02	0.2	0.269	1800	3000	2010	1.125241
3	637.5	496.65	622.56	727.359	829.758	728.899	0.02	0.2	0.221	1800	3000	1800	1.140782
4	650.0	485.18	642.55	649.783	630.704	649.783	0.02	0.2	0.209	1800	3000	1800	0.970638
5	650.7	499.91	670.44	651.435	636.052	651.435	0.02	0.2	0.179	1800	3000	1800	0.976386
6	649.0	482.25	607.85	646.547	626.06	646.547	0.02	0.2	0.259	1800	3000	1800	0.968313
7	649.0	520.49	590.47	621.507	787.759	646.133	0.02	0.2	0.300	1800	3000	1998	1.267498
8	486.5	511.41	591.6	478.138	630.383	479.578	0.02	0.2	-0.036	1800	3000	1866	1.318412
9	179.6	497.16	639.15	424.131	480.359	423.966	0.02	0.2	-0.300	1800	3000	1800	1.132572
10	583.4	501.62	668.06	585.677	699.037	585.677	0.02	0.2	0.108	1800	3000	1800	1.193554
11	301.5	506.75	663.88	430.644	466.263	430.631	0.02	0.2	-0.215	1800	3000	1800	1.082711
12	641.6	483.13	614.33	639.559	622.25	639.559	0.02	0.2	0.237	1800	3000	1800	0.972936
13	611.7	481.93	615.42	612.28	596.116	612.28	0.02	0.2	0.195	1800	3000	1800	0.9736
14	649.0	512.63	668.43	650.241	634.528	650.241	0.02	0.2	0.178	1800	3000	1800	0.975835
15	237.0	438.7	549.29	386.305	389.685	386.305	0.02	0.2	-0.300	1800	3000	1800	1.00875
16	578.6	488.86	619.55	580.045	577.557	580.045	0.02	0.2	0.144	1800	3000	1800	0.995711
17	285.5	491.68	602.67	415.366	408.897	415.366	0.02	0.2	-0.300	1800	3000	1800	0.984426
18	455.3	516.04	563.3	459.254	479.54	469.011	0.02	0.2	-0.211	1800	3000	1800	1.044172
19	620.7	525.3	601.44	617.031	712.818	622.858	0.02	0.2	0.246	1800	3000	1846	1.155239
20	628.9	499.25	605.57	620.681	691.324	639.1	0.02	0.2	0.239	1800	3000	1939	1.113815
21	477.4	473.72	580.03	490.906	468.196	490.759	0.02	0.2	0.026	1800	3000	1800	0.953739
22	616.6	515.51	658.49	632.698	628.87	631.239	0.02	0.2	0.147	1800	3000	1800	0.99395
23	696.7	491.68	625.84	667.923	663.681	667.923	0.02	0.2	0.295	1800	3000	1800	0.993649
24	486.0	622.6	705.45	568.485	456.181	493.622	0.02	0.2	-0.277	1800	3000	2681	0.80245
25	576.7	506.66	680.95	578.46	576.879	578.46	0.02	0.2	0.092	1800	3000	1800	0.997267
26	632.5	500.21	671.01	633.494	619.732	633.494	0.02	0.2	0.159	1800	3000	1800	0.978276
27	465.5	467.03	583.09	497.441	475.131	495.957	0.02	0.2	0.018	1800	3000	1800	0.95515
28	570.0	501.87	635.49	572.371	565.55	572.371	0.02	0.2	0.112	1800	3000	1800	0.988083
29	616.3	482.43	608.21	616.178	599.355	616.178	0.02	0.2	0.212	1800	3000	1800	0.972698
30	298.3	513.07	590.51	455.755	522.067	455.755	0.02	0.2	-0.300	1800	3000	1800	1.145499
31	360.0	511.53	556.25	439.706	562.215	436.649	0.02	0.2	-0.300	1800	3000	1800	1.278616
32	588.4	522.23	593.09	589.089	678.907	589.089	0.02	0.2	0.188	1800	3000	1800	1.152469
33	652.5	515.03	594.58	629.665	742.287	662.644	0.02	0.2	0.300	1800	3000	2043	1.17886
34	637.2	501.51	627.54	636.35	636.746	636.35	0.02	0.2	0.214	1800	3000	1800	1.000622
35	209.4	510.29	670.7	414.301	434.193	414.301	0.02	0.2	-0.300	1800	3000	1800	1.048013
36	184.9	480.66	628.73	398.288	449.661	396.819	0.02	0.2	-0.300	1800	3000	1800	1.128985
37	207.5	486.43	638.51	416.397	485.209	416.39	0.02	0.2	-0.300	1800	3000	1800	1.165256
38	545.6	512.66	677.2	547.35	664.404	547.351	0.02	0.2	0.056	1800	3000	1800	1.213856
39	664.7	508.74	666.29	664.793	706.41	664.792	0.02	0.2	0.198	1800	3000	1800	1.062601
40	637.0	456.3	564.53	606.986	615.78	606.986	0.02	0.2	0.300	1800	3000	1800	1.014488
41	693.3	502.89	640.27	673.75	673.176	673.75	0.02	0.2	0.269	1800	3000	1800	0.999148
42	648.6	481.45	613.02	645.629	629.648	645.629	0.02	0.2	0.249	1800	3000	1800	0.975247
43	570.0	552.36	667.61	624.276	438.616	615.262	0.02	0.2	0.048	1800	3000	2151	0.702599
44	740.0	500.05	619.02	677.96	653.049	677.96	0.02	0.2	0.300	1800	3000	1800	0.963256
45	587.2	462.23	582.28	585.94	557.779	585.937	0.02	0.2	0.207	1800	3000	1800	0.951939
46	605.0	490.86	628	612.703	595.256	612.703	0.02	0.2	0.170	1800	3000	1800	0.971525
47	252.3	485.1	607.58	391.67	385.411	391.67	0.02	0.2	-0.300	1800	3000	1800	0.98402
48	264.2	430.2	546.76	377.111	380.724	377.111	0.02	0.2	-0.236	1800	3000	1800	1.009581

49	286.0	439.36	549.98	394.451	398.312	394.451	0.02	0.2	-0.230	1800	3000	1800	1.009788
50	604.1	488.25	619.33	604.705	599.322	604.705	0.02	0.2	0.179	1800	3000	1800	0.991098
51	701.3	491.95	603.01	661.773	645.766	661.773	0.02	0.2	0.300	1800	3000	1800	0.975812
52	330.9	469.66	599.5	420.334	443.618	419.923	0.02	0.2	-0.172	1800	3000	1800	1.055394
53	432.6	516.12	566.41	429.731	463.37	429.731	0.02	0.2	-0.279	1800	3000	1800	1.078279
54	495.8	520.77	591.44	485.963	526.666	485.963	0.02	0.2	-0.043	1800	3000	1800	1.083757
55	610.0	512.04	592.45	606.233	715.413	612.508	0.02	0.2	0.239	1800	3000	1841	1.180096
56	198.4	470.45	626.37	395.52	423.044	395.52	0.02	0.2	-0.294	1800	3000	1800	1.069589
57	345.6	511.74	676.46	441.109	434.739	441.109	0.02	0.2	-0.162	1800	3000	1800	0.985559
58	228.0	486.9	608.81	394.473	388.224	394.473	0.02	0.2	-0.300	1800	3000	1800	0.984159
59	280.8	430.03	546.61	380.589	384.336	380.589	0.02	0.2	-0.210	1800	3000	1800	1.009845
60	495.4	488.32	619.5	496.068	497.001	496.068	0.02	0.2	0.030	1800	3000	1800	1.001881
61	186.0	438.87	555.98	375.039	371.242	398.599	0.02	0.2	-0.300	1800	3000	1800	0.989876
62	296.7	518.12	570.78	428.763	457.266	428.763	0.02	0.2	-0.300	1800	3000	1800	1.066477
63	131.4	509.94	670.94	413.471	409.621	413.471	0.02	0.2	-0.300	1800	3000	1800	0.990689
64	162.2	470.86	719.98	408.346	440.465	408.346	0.02	0.2	-0.203	1800	3000	1800	1.078656
65	192.0	486.61	608.88	393.297	387.038	393.297	0.02	0.2	-0.300	1800	3000	1800	0.984086
66	205.7	430.66	547.38	369.365	372.293	369.365	0.02	0.2	-0.300	1800	3000	1800	1.007927
67	110.1	490.67	608.8	491.885	393.004	505.749	0.02	0.2	-0.300	1800	3000	3000	0.798975
68	256.3	433.38	550.08	398.903	370.67	398.903	0.02	0.2	-0.253	1800	3000	1800	0.929223
69	589.6	515.7	566.53	591.412	708.289	591.427	0.02	0.2	0.282	1800	3000	1800	1.197624
70	199.4	468.67	717.42	411.01	441.566	411.01	0.02	0.2	-0.175	1800	3000	1800	1.074344
71	345.2	429.07	545.75	394.421	398.53	394.421	0.02	0.2	-0.109	1800	3000	1800	1.010418
72	356.7	443.98	558.28	404.298	401.641	404.298	0.02	0.2	-0.117	1800	3000	1800	0.993428
73	356.5	518.06	571.02	428.636	447.52	428.636	0.02	0.2	-0.300	1800	3000	1800	1.044056
74	182.9	509.02	670.2	412.533	408.931	412.534	0.02	0.2	-0.300	1800	3000	1800	0.991269
75	170.5	469.56	718.8	408.137	439.354	408.137	0.02	0.2	-0.196	1800	3000	1800	1.076487
76	194.2	483.98	607.19	389.35	383.042	389.35	0.02	0.2	-0.300	1800	3000	1800	0.983799
77	239.8	430.56	547.26	372.407	375.569	372.407	0.02	0.2	-0.274	1800	3000	1800	1.008491
78	247.4	462.5	594.36	487.626	360.059	501.244	0.02	0.2	-0.274	1800	3000	3000	0.738392
79	142.6	444.14	558.88	401.084	376.338	401.084	0.02	0.2	-0.300	1800	3000	1800	0.938302
80	123.5	552.37	677.72	508.883	468.538	355.213	0.02	0.2	-0.300	1800	3000	1800	0.920719
81	169.6	299.14	453.87	242.329	252.017	242.329	0.02	0.2	-0.131	1800	3000	1800	1.039979
82	224.0	354.81	476.21	316.98	245.315	245.72	0.02	0.2	-0.174	1800	3000	3000	0.773913
83	144.4	292.48	457.83	232.748	243.554	232.748	0.02	0.2	-0.141	1800	3000	1800	1.046428
84	139.0	488.52	676.54	465.795	337.397	442.469	0.02	0.2	-0.300	1800	3000	3000	0.724347
85	113.5	299.85	454.17	228.78	235.636	228.78	0.02	0.2	-0.197	1800	3000	1800	1.029968
86	202.9	356.86	477.44	316.129	230.392	230.392	0.02	0.2	-0.210	1800	3000	3000	0.728791
87	126.0	300.19	462.6	234.974	245.04	234.974	0.02	0.2	-0.173	1800	3000	1800	1.042839
88	210.9	528.3	674.87	371.944	281.844	442.091	0.02	0.2	-0.300	1800	3000	3000	0.757759
89	534.8	301.14	454.79	532.234	544.267	532.234	0.02	0.2	0.294	1800	3000	1800	1.022608
90	234.0	348.56	470.82	312.806	213.411	213.528	0.02	0.2	-0.149	1800	3000	2751	0.682247
91	372.4	311.5	469.61	372.941	390.609	372.941	0.02	0.2	0.089	1800	3000	1800	1.047375
92	181.2	473.36	676.4	344.836	267.529	335.215	0.02	0.2	-0.239	1800	3000	3000	0.775815
93	260.9	299.48	454	272.993	284.423	272.993	0.02	0.2	-0.025	1800	3000	1800	1.041869
94	230.4	357.03	477.59	319.583	239.275	239.275	0.02	0.2	-0.169	1800	3000	3000	0.74871
95	234.1	300.36	462.78	264.043	276.752	264.043	0.02	0.2	-0.053	1800	3000	1800	1.048132
96	771.4	301.69	455.05	537.219	549.331	537.219	0.02	0.2	0.300	1800	3000	1800	1.022546
97	639.5	312.36	470.08	555.163	579.478	555.163	0.02	0.2	0.300	1800	3000	1800	1.043798
98	1293.3	312.41	470.11	555.184	579.5	555.184	0.02	0.2	0.300	1800	3000	1800	1.043798
99	275.1	513.86	594.45	391.479	519.7	391.479	0.02	0.2	-0.300	1800	3000	1800	1.32753
100	264.9	518.35	571.54	428.757	435.856	428.757	0.02	0.2	-0.300	1800	3000	1800	1.016557
101	264.1	497.55	662.14	412.841	410.828	412.841	0.02	0.2	-0.235	1800	3000	1800	0.995124
102	157.3	470.2	651.94	394.609	419.606	394.609	0.02	0.2	-0.290	1800	3000	1800	1.063346
103	300.1	483.3	607.02	401.34	396.767	401.34	0.02	0.2	-0.247	1800	3000	1800	0.988606
104	183.6	430.32	547.12	368.836	371.75	368.836	0.02	0.2	-0.300	1800	3000	1800	1.007901
105	287.7	479.39	606.5	425.794	389.801	387.93	0.02	0.2	-0.251	1800	3000	1800	0.915469
106	174.1	438.7	554.77	398.116	370.274	397.293	0.02	0.2	-0.300	1800	3000	1800	0.930066
107	296.1	488.65	624.87	406.411	395.889	406.411	0.02	0.2	-0.234	1800	3000	1800	0.97411
108	123.3	469.35	677.14	413.382	264.409	271.348	0.02	0.2	-0.280	1800	3000	3000	0.639624
109	259.3	301.14	455.32	273.371	284.953	273.371	0.02	0.2	-0.029	1800	3000	1800	1.042367
110	540.5	306.32	536.95	436.485	444.162	436.48	0.02	0.2	0.203	1800	3000	1800	1.017588
111	320.7	355.08	476.28	334.102	268.144	331.001	0.02	0.2	-0.031	1800	3000	2043	0.802581
112	657.6	312.28	470.58	555.95	580.421	555.95	0.02	0.2	0.300	1800	3000	1800	1.044017
113	166.6	509.79	671.05	413.196	409.672	413.196	0.02	0.2	-0.300	1800	3000	1800	0.991471
114	177.6	485.44	608.29	391.283	384.988	391.283	0.02	0.2	-0.300	1800	3000	1800	0.983912
115	219.0	489.4	609.34	491.743	391.71	496.475	0.02	0.2	-0.300	1800	3000	3000	0.796575
116	255.8	500.33	632.15	406.247	392.58	406.247	0.02	0.2	-0.300	1800	3000	1800	0.966358
117	250.8	467.94	676.46	424.3	274.057	274.057	0.02	0.2	-0.167	1800	3000	3000	0.645904
118	408.4	300.14	454.46	408.893	421.162	408.893	0.02	0.2	0.146	1800	3000	1800	1.030005
119	465.4	294.79	533.76	383.182	388.843	383.181	0.02	0.2	0.148	1800	3000	1800	1.014774
120	319.5	354.49	475.61	255.851	266.24	288.025	0.02	0.2	-0.032	1800	3000	1800	1.040606

121	568.8	251.99	419.22	507.98	535.815	507.98	0.02	0.2	0.300	1800	3000	1800	1.054795
122	464.1	264	438.97	463.787	485.258	463.787	0.02	0.2	0.226	1800	3000	1800	1.046295
123	176.1	508.82	671.02	411.601	408.369	411.601	0.02	0.2	-0.300	1800	3000	1800	0.992148
124	228.9	484.12	607.95	388.299	381.942	388.299	0.02	0.2	-0.300	1800	3000	1800	0.983629
125	411.6	444.96	571.97	453.44	419.386	453.508	0.02	0.2	-0.027	1800	3000	1800	0.924899
126	352.8	487.81	610.84	415.402	420.34	415.402	0.02	0.2	-0.177	1800	3000	1800	1.011887
127	262.1	500.33	632.42	405.558	391.767	405.558	0.02	0.2	-0.300	1800	3000	1800	0.965995